Protective effect of quercetin on high-fat diet-induced non-alcoholic fatty liver disease in mice is mediated by modulating intestinal microbiota imbalance and related gut-liver axis activation

David Porras[a], Esther Nistal[a], Susana Martínez-Flórez[a], Sandra Pisonero-Vaquero[a], José Luis Olcoz[b,c] ,Ramiro Jover[b,d,e], Javier González-Gallego[a,b] , María Victoria García-Mediavilla[a,b], and Sonia Sánchez-Campos[a,b*]

[*]MVGM and SSC share senior authorship

[a]Institute of Biomedicine (IBIOMED), University of León, León, Spain; [b]Centro de Investigación Biomédica en Red de Enfermedades Hepáticas y Digestivas (CIBERehd), Instituto de Salud Carlos III, Madrid, Spain; [c]Department of Gastroenterology. Complejo Asistencial Universitario de León, León, Spain; [d]Experimental Hepatology Unit, IIS Hospital La Fe, Valencia, Spain; [e]Department of Biochemistry and Molecular Biology, University of Valencia, Valencia, Spain.

David Porras: dporrs00@estudiantes.unileon.es

Esther Nistal: esthernistal@hotmail.com

Susana Martínez-Flórez: smarf@unileon.es

Sandra Pisonero-Vaquero: spisv@unileon.es

José Luis Olcoz: jolcozg@gmail.com

Ramiro Jover: ramiro.jover@uv.es

Javier González-Gallego: jgonga@unileon.es

María Victoria García Mediavilla: mvgarm@unileon.es

Sonia Sánchez-Campos: ssanc@unileon.es

Correspondence: Sonia Sánchez-Campos, Institute of Biomedicine, University of León, Campus de Vegazana, 24071 León, Spain.

E-mail: ssanc@unileon.es

Fax: +34987291267

Abbreviations: ALT, alanine aminotransferase; C/EBPα, CCAAT/enhancer binding protein alpha; CHOP, CCAAT-enhancer-binding protein homologous protein; CYP2E1, cytochrome P450 2E1; DAMPs, danger-associated molecular patterns; FABP1, fatty acid binding protein 1; FAS, fatty acid synthase; FAT/CD36, fatty acid translocase CD36; FFA, free fatty acid; FOXA1, forkhead box protein A1; GAPDH, glyceraldehyde-3-phosphate dehydrogenase; GRP78, 78 kDa glucose-regulated protein; HFD, high fat diet; HOMA-IR, homeostasis model assessment of insulin resistance; IAP, intestinal phosphatase alkaline; IL-6, interleukin 6; LPO, lipid peroxidation; LPS, lipopolysaccharide; LXRα, liver X receptor alpha; NAFLD, non-alcoholic fatty liver disease; NAS, NAFLD activity score; NASH, non-alcoholic steatohepatitis; NF-κB , nuclear factor kappa B; NLRP3, NOD-like receptor family pyrin domain containing 3; PAMPs, pathogen-associated molecular patterns; PRRs, pattern recognition receptors; SCFAs, short-chain fatty acids; SREBP-1c, sterol regulatory element binding protein 1c; TG, triglycerides; TLR, Toll-like receptor; TNF-α; tumor necrosis factor; UPR, unfolded protein response.

Abstract

Gut microbiota is involved in obesity, metabolic syndrome and the progression of nonalcoholic fatty liver disease (NAFLD). It has been recently suggested that the flavonoid quercetin may have the ability to modulate the intestinal microbiota composition, suggesting a prebiotic capacity which highlights a great therapeutic potential in NAFLD. The present study aims to investigate benefits of experimental treatment with quercetin on gut microbial balance and related gut-liver axis activation in a nutritional animal model of NAFLD associated to obesity. C57BL/6J mice were challenged with high fat diet (HFD) supplemented or not with quercetin for 16 weeks. HFD induced obesity, metabolic syndrome and the development of hepatic steatosis as main hepatic histological finding. Increased accumulation of intrahepatic lipids was associated with altered gene expression related to lipid metabolism, as a result of deregulation of their major modulators. Quercetin supplementation decreased insulin resistance and NAFLD activity score, by reducing the intrahepatic lipid accumulation through its ability to modulate lipid metabolism gene expression, cytochrome P450 2E1 (CYP2E1)-dependent lipoperoxidation and related lipotoxicity. Microbiota composition was determined via 16S ribosomal RNA Illumina next-generation sequencing. Metagenomic studies revealed HFD-dependent differences at phylum, class and genus levels leading to dysbiosis, characterized by an increase in *Firmicutes/Bacteroidetes* ratio and in Gram-negative bacteria, and a dramatically increased detection of *Helicobacter* genus. Dysbiosis was accompanied by endotoxemia, intestinal barrier dysfunction and gut-liver axis alteration and subsequent inflammatory gene overexpression. Dysbiosis-mediated toll-like receptor 4 (TLR-4)-NF-κB signaling pathway activation was associated with inflammasome initiation response and reticulum stress pathway induction. Quercetin reverted gut microbiota imbalance and related

endotoxemia-mediated TLR-4 pathway induction, with subsequent inhibition of inflammasome response and reticulum stress pathway activation, leading to the blockage of lipid metabolism gene expression deregulation. Our results support the suitability of quercetin as a therapeutic approach for obesity-associated NAFLD via its anti-inflammatory, antioxidant and prebiotic integrative response.

Keywords: CYP2E1; dysbiosis; endoplasmic reticulum stress; gut-liver axis; inflammasome; inflammation; intestinal barrier function; intestinal microbiota; lipid metabolism; lipotoxicity; NAFLD; quercetin.

Introduction

Nonalcoholic fatty liver disease (NAFLD) is the commonest form of liver disease in the Western countries [1]. NAFLD is associated with obesity and represents the hepatic manifestation of metabolic syndrome [2]. It ranges from simple hepatic lipid accumulation (steatosis) to steatohepatitis (NASH) when combined with inflammation, which can lead to cirrhosis, hepatocellular carcinoma and death related to liver morbidity [3]. Despite advances in this field, the molecular mechanisms of progression from steatosis to NASH remain obscure. The current and most accepted theory proposed for understanding the pathogenesis of NAFLD is the multiple parallel hits hypothesis. The "multiple hit" hypothesis conceives a complex interplay between multiple events acting in parallel with genetic predisposition, providing a more accurate explanation of the pathogenic mechanisms involved in NAFLD. Thus, NAFLD development and progression depend on changes in lipid metabolism, derived from the induction of fatty acid biosynthesis and transport that contributes to the intrahepatic lipid accumulation associated with insulin resistance, accompanied by oxidative stress-mediated lipotoxicity and proinflammatory cytokines gene expression, among others mechanisms [4-6].

A relationship has been reported between intestinal microbiota dysbiosis, barrier function and immune response and liver diseases [4, 7]. Thus, gut microbiota is involved in obesity, metabolic syndrome and in the progression of NAFLD [8-10]. In NAFLD, alteration of gut microbiota and increased intestinal permeability enhance exposure of the liver to gut-derived bacterial products inducing chronic endotoxemia and associated gut-liver axis alteration [8, 10]. Thereby, gut microbiota composition determination adds information to classical predictions of NAFLD severity and suggests novel targets for pre/probiotics therapies [11]. In this respect, it has been described that

gut microbiota modulation with prebiotics improved obesity, metabolic syndrome and fatty liver [12].

Previous studies have established the modulatory capacity of polyphenols on the gut microbial community [13-15]. Natural compounds with antioxidant and anti-inflammatory capacity present in the diet such as flavonoids, including quercetin, appear to be capable of reducing hepatic lipid accumulation, which gives them a great therapeutic potential in NAFLD [5]. Recently, it has been indicated that quercetin may have the ability to modify the gut microbial balance [16], suggesting a prebiotic capacity. Thus, the use of flavonoids as quercetin in NAFLD might be considered as a potential strategy to modulate intestinal bacterial composition.

The present study aimed to investigate the potential benefits of the experimental treatment with quercetin on HFD-fed mice restoring host-microbial balance and regulating endotoxemia-related immune-mediated inflammatory signaling mechanisms and lipid metabolism alteration in the pathogenesis of nonalcoholic liver disease. Our results would enable the design of quercetin administration-based novel therapeutic approaches to manipulate gut microbiota to treat obesity-associated NAFLD.

Materials and methods

Animals and treatments

Seven-weeks-old male C57BL/6J mice were fed with a standard diet to their adaptation to the environment and later distributed in 4 groups (10 mice per group) according with the following diets (Research Diets, Inc. New Brunswick, NJ. USA): (1) Control (10% of energy from fat; D12450J); (2) Control Q (10% of energy from fat + 0.05% (wt/wt) aglycone quercetin D14062801) (3) HFD (60% energy from fat; D12492) and (4) HFDQ (60% energy from fat + 0.05% (wt/wt) aglycone quercetin; D14062802). Mice were fed freely available diets and water, and housed under controlled conditions of temperature, humidity and lighting. Body weight and food intake were monitored weekly. After 16 weeks, mice were euthanized, plasma, liver, small intestine and adipose tissue samples were collected and weighed. The right posterior lobe of the liver was fixed in 10% formalin and the remaining liver was snap frozen.

All procedures were approved by the local Animal Ethics Committees in accordance with the European Research Council guidelines for animal care and use.

Histopathology and fluorescence microscopy

Formalin-fixed and paraffin-embedded liver samples were sectioned and stained with hematoxylin and eosin (H&E). Lesions were evaluated by a histological scoring system for non-alcoholic fatty liver disease proposed by Kleiner *et al.* [17]. The NAFLD activity score (NAS) was used as a tool to provide a numerical score evaluating semi-quantitatively 3 histological features: steatosis (0-3), lobular inflammation (0-3) and hepatocellular ballooning (0-2). Samples with scores more than 5 were correlated with a diagnosis of NASH, and score less than 3 were diagnosed as “not NASH.” Histological analysis was measured by two objective expert examiners blinded to experimental

design protocol. Frozen liver tissue samples were sectioned and stained with 1 μg/ml Bodipy 493/503 and Bodipy 581/591 C11 (Invitrogen, Carlsbad, CA, USA) combined with DAPI for nuclei staining, to analyze lipid accumulation or lipoperoxidation (LPO), respectively. The sections were imaged using a Nikon Eclipse Ti inverted microscope (Nikon, Amstelveen, The Netherlands).

Biochemical analysis

Plasma levels of triglycerides (TG), and alanine aminotransferase activity (ALT) were analyzed by the Instrumental Techniques Laboratory of the University of León using standard techniques. Plasma levels of insulin and interleukin (IL)-6 were determined by specific ELISA kits according to the manufacturer's instructions (Millipore, Darmstadt, Germany). Plasma glucose levels were measured with the Accu-Chek (Roche Diagnostics, Almere, The Netherlands) after an 8-hour fast. The homeostasis model assessment of insulin resistance (HOMA-IR) was used to calculate the insulin resistance using the formula:

HOMA-IR = Fasting glucose (mg/dl) × Fasting insulin (μU/ml) /405

Plasma endotoxemia

Plasma lipopolysaccharide (LPS) and ethanol quantification were performed following the instructions of the commercial kits (LAL Chromogenic Endotoxin Quantification Kit, Thermo Scientific, and Ethanol Colorimetric Assay Kit, Biovision, respectively).

Measurement of liver triglycerides and free fatty acids

Triglycerides and free fatty acids (FFA) levels in the hepatic tissue were analyzed after liver homogenization following the guide provided by the company Biovision Research Products (Mountain View, CA, USA).

Caecal content collection

Caecal samples were collected immediately after euthanasia and gathered in 2 ml *Eppendorf* tubes and immediately frozen at -80ºC for future analysis.

Caecal short-chain fatty acids (SCFAs) identification and quantification

Samples were analyzed as previously described [18] using 4-methylvaleric as internal standard. The caecal samples were suspended and homogenised in water. After centrifugation for 10 min at 12.000 rpm, the supernatant was recollected and acidified by addition of HCl. The internal standard was added into the supernatant at a final concentration of 258 μM. SCFAs were identified and quantized on a gas chromatograph CP-3800 (Varian) connected to a mass spectrometry (GC-MS) (Saturn. Varian). Data were collected using the Varian MS Workstation (version 6.9.2.) software. The linear regression equation ($R^2 \geq 0.99$) was used to calculate the concentration of each SCFA from the standard curves obtained with seven different concentrations.

DNA extraction, PCR and pyrosequencing

Caecal samples were selected to pyrosequencing analysis. The extraction of genomic DNA from caecal samples were carried out using the QIAamp DNA Stool Mini Kit (Qiagen, Hilden, Germany) according to the manufacture's instruction, with some modifications, as follows: an initial bead beating step was included and the lysis temperature was increased from the recommended 70 to 90°C to aid in the recovery of

DNA from bacteria that are difficult to lyse. The DNA concentration was determined using a NanoDrop ND-1000 spectophotometer (Saveen& Werner, Limhann, Sweden) and stored at -20ºC until analysis.

Amplification of the 16S rRNA V3-V4 hypervariable region was carried out using the 16S V3 314F forward (5'TCGTCGGCAGCGTCAGATGTGTATAAGAGACAGCCTACGGGNGGCWGCAG3') and V4 805R reverse primer (5'GTCTCGTGGGCTCGGAGATGTGTATAAGAGACAGGACTACHVGGGTATCTAATCC3') [19] with added Illumina adapter overhang nucleotide sequences. The PCR conditions used were 3 min at 95ºC, followed by 25 cycles of 30 s at 95ºC, 30 s at 55ºC and 30 s at 72ºC, and a final extension at 72ºC for 5 min. Each reaction mixture (25µl) contained 50 ng of genomic DNA, 0.5 µl of amplicon PCR forward primer (0.2 µM), 0.5 µl of amplicon PCR reverse primer (0.2 µM) and 12.5 µl of 2x KAPA HifiHotStart Ready Mix (Kapa Biosystems, Wilmington, MA, USA) Three PCR products per sample were pooled and purified with the Wizard® Genomic DNA Purification Kit (Promega, Madison, WI, USA).

According to the manufacturer's protocol, each reaction was cleaned up with AgencourtAMPure XP beads (Beckman Coulter Genomics, Danvers, MA, USA). Attachment of dual indices and Illumina sequencing adapters was performed using 5 µl of amplicon PCR product DNA, 5 µl of Illumina Nextera XT Index Primer 1 (N7xx), 5 µl of Nextera XT Index Primer 2 (S5xx), 25 µl of 2x KAPA HiFiHotStart Ready Mix, and 10 µl of PCR-grade water (UltraClean DNA-free PCR water; MO BIO Laboratories, Inc., Carlsbad, CA, USA); in this case, amplification was carried out under the following conditions: 3 min at 95°C, followed by 8 cycles of 30 s at 95°C, 30 s at 55°C, and 30 s at 72°C, and a final extension at 72°C for 5 min. Constructed 16S

metagenomic libraries were purified with AgencourtAMPure XP beads and quantified with Quant-iTPicoGreen (Kapa Biosystems). Library quality control and average size distribution was determined with the Agilent Technologies 2100 Bioanalyzer. Libraries were normalized and pooled to 40 nM based on quantified values. Pooled samples were denatured and diluted to a final concentration of 6pM with a 30% PhiX (Illumina) control. Amplicons were subjected to pyrosequencing using the MiSeq Reagent Kit V3 in the Illumina MiSeq System.

Bioinformatic analysis

The online portal for Illumina data analysis (http://www.illumina.com/) was used to access Basespace at https://basespace.illumina.com/home/index, and the 16Smetagenomics Basespace application was applied to the data. 16S metagenomics analysis uses DNA from amplicon sequencing of prokaryotic 16S small subunit rRNA genes with the high performance version of RDP Naïve Bayes algorithm [20]. FASTQ sequences were uploaded to Basespace and the 16S metagenomics application was executed. After assembling, full length sequences from paired ends were referenced against the Illumina curated version of Green genes data base (May 2013) at 97% identity level. The groups of related DNA sequences were assigned to operational taxonomic units (OTUs). These OTUs were analyzed with the Vegan package [21] in R software (R Development Core Team, 2011) to estimate the alpha and beta diversity of the samples.

Quantitative Real-Time PCR

For total bacteria concentration determination, DNA was extracted from caecal samples. Samples were analyzed by real-time PCR. Primer sets and real-time PCR conditions

used to amplify bacterial 16S rRNA genes are listed in Table 1. For quantification of these different target organisms, the StepOnePlus Real-Time PCR system (Applied Biosystems, Weiterstadt, Germany) was used. The amplification reaction was carried out with 50 ng of DNA template in a final volume of 20 µl, 0.3 µM of each forward and reverse primer, and 10 µl of LightCycler-Fast Start DNA Master SYBR Green (Roche Diagnostics). The following PCR protocol was run: 95ºC (10 min), then 95ºC (15 s), variable annealing temperature (60 s) for 40 cycles. Each sample was run in triplicate and quantitative PCR standards were created by amplifying the target 16S rRNA genes from appropriate positive control strains. Standard curves were then generated for each bacterial group and used to calculate the concentration of each sample.

To determine relative gene expression in liver samples, Trizol reagent (Life Technologies) was used to isolate the total RNA. First-strand cDNA was amplified using High-Capacity cDNA Archive Kit (Applied Biosystems). Multiplex real-time PCR reactions on a StepOne Plus (Applied Biosystems) was used to synthesize cDNA [22]. TaqMan primers and probes were derived from the commercially available TaqMans® Gene Expression Assays (Applied Biosystems) (Table 2). The $2^{-\Delta\Delta Ct}$ method was applied to determinate relative changes in gene expression levels. Glyceraldehyde-3-phosphate dehydrogenase (GAPDH) was used to normalize the cycle number at which the transcripts were detectable (Ct) referred to as ΔCt. PCR efficiency was determined by TaqMan analysis on a standard curve for targets and endogenous control amplifications that were highly similar.

Western blot

Protein extraction and Western blotting were performed as described [5], using rabbit polyclonal antibodies against fatty acid synthase (FAS) (Santa Cruz Biotechnology,

Santa Cruz, CA, USA), nuclear factor kappa B (NF-κB) p65 subunit (Santa Cruz), toll-like receptor 4 (TLR-4) (Abcam, Cambridge, UK), NOD-like receptor family pyrin domain containing 3 (NLRP3) (Cell Signaling, MA, USA), caspase 1 (Cell Signaling), 78 kDa glucose-regulated protein (GRP78) (Abcam) and CCAAT-enhancer-binding protein homologous protein (CHOP) (Santa Cruz Biotechnology), claudin-1 (Abcam), occludin (Abcam), and intestinal alkaline phosphatase (IAP) (Abcam). Primary antibody binding was detected using an appropriate anti-rabbit secondary antibody conjugated with horseradish peroxidase (DAKO, Glostrup, Denmark), and detected with chemiluminescence detection system (ECL kit, Amersham Pharmacia, Uppsala, Sweden). The intensity of the bands was quantified using a densitometry quantification program (Scion Image, Frederick, MD, USA).

Statistical analysis

Data are expressed as the mean ± SEM. Significant differences were evaluated by one way analysis of variance (ANOVA) and Newman–Keul's test or Pearson's correlation. $p<0.05$ was considered to be significant for a difference. From gut microbiota composition data statistical significance was determined by nonparametric Kruskal-Wallis test followed by Mann-Whitney U test when $p<0.05$. All statistical analyses were performed using SPSS 22.0 software (Chicago, IL, USA).

Results

Quercetin ameliorates features of metabolic syndrome and histological findings in mice with HFD-induced NAFLD

Because of the lack of significant differences between results obtained in Control and ControlQ mice, the group without quercetin treatment was considered as Control group.

To examine the effects of quercetin on non-alcoholic fatty liver disease male C57BL/6 mice were subjected to HFD with or without quercetin supplementation for 16 weeks. As previously described [23], in our *in vivo* model of NAFLD high fat diet feeding induced body weight gain, increased epididymal fat accumulation and developed hallmark characteristic of metabolic syndrome as elevated fasting blood glucose and insulin, and HOMA-IR (+52%, +328%, +537%, respectively, *vs* Control) (Table 3). Quercetin administration culminated with a reduction on body weight gain, epididymal fat accumulation, and liver weight, without differences in food intake, in comparison with HFD-fed mice (-23%, -31%, -17%, respectively) (Table 3). In addition, quercetin supplementation induced a significant reduction in fasting glucose and insulin levels, improving insulin sensitivity as reflected in HOMA-IR, compared to HFD group (-10%, -30%, -36%, respectively) (Table 3).

After 16 weeks, mice fed with HFD diet showed significantly higher plasma triglyceride and ALT levels in comparison with control mice (+46%, +208%, respectively) (Table 3), which were significantly reduced by quercetin supplementation (TG: -28% and ALT: -35%, respectively, *vs* HFD) (Table 3).

As shown in Fig. 1A, histopathological assessment of HFD-fed mice liver disclosed microvesicular and macrovesicular steatosis in hepatocytes, indicative of disturbed lipid metabolism. Slight liver inflammation and ballooning were also observed in HFD-fed

mice, leading to a 10-fold increased NAFLD activity score, compared with control mice (Fig. 1B). Quercetin-treated mice exhibited significantly less fat deposition, inflammation and balloning in hepatocytes, resulting in a reduced NAS (-46%, *vs* HFD) (Fig.1B).

Confirming histological features, Bodipy 496/503 staining analysis revealed a significant increase of hepatic lipid accumulation in mice fed with high fat diet compared to control mice. These results were correlated with increased hepatic trygliceride and free fatty acid contents in HFD-fed mice (+185% and +94%, respectively, *vs* Control) (Fig. 1D and E). Quercetin supplementation was able to decrease steatosis, showing a reduction of liver lipid droplets (Fig. 1C) associated with a diminished hepatic TG and FFA accumulation in comparison to HFD-fed mice (-28% and -28%, respectively) (Fig. 1D and E).

Quercetin decreases CYP2E1-mediated lipid peroxidation in mice with HFD-induced NAFLD

Given its ability to generate oxidative stress and subsequent lipoperoxidation, cytochrome P450 (CYP)2E1 is a key factor in the pathogenesis of fatty liver disease. In our in vivo model of NAFLD we found that HFD-fed mice showed a large increase in lipid peroxidation compared to control mice (Fig.1C), that was accompanied with a significantly increased CYP2E1 gene expression (+67%, *vs* Control) (Fig 1F). Quercetin treatment was able to counteract LPO induction in parallel with the reduction of CYP2E1 overexpression (-15%, *vs* HFD) (Fig. 1C and F).

Quercetin supplementation prevents lipid metabolism-related gene expression deregulation in mice with HFD-induced NAFLD

We next assessed the effect of high fat diet on the expression of genes involved in *de novo* lipogenesis, including liver X receptor (LXR)α, sterol regulatory element binding protein (SREBP)-1c and FAS, and fatty acid uptake and trafficking, as fatty acid binding protein (FABP)1 and fatty acid translocase CD36 (FAT/CD36). As shown in Fig. 2A and B, the relative mRNA expression of LXRα and its lipogenic downstream target genes was increased in HFD-fed mice compared to control mice (LXRα: +20%, SREPB-1c: +36%, and FAS: +36%), while quercetin supplementation reverted de novo lipogenesis gene overexpression (-20%, -26% and -23%, respectively, *vs* HFD group). As expected, a similar trend of upregulation of FAS protein was observed in HFD-fed mice (+144%, *vs* Control), which was attenuated by oral supplementation with quercetin (-28%, *vs* HFD group) (Fig. 2C). Regarding to gene expression of fatty acid uptake- and trafficking-related genes, as show in Fig. 2A, we found that HFD feeding induced a significant overexpression of FAT/CD36 (+136%) and FABP1 downregulation (-20%), compared with control mice. The hepatic gene expression of their regulatory transcription factors forkhead box protein A1 (FOXA1) and CCAAT/enhancer-binding protein alpha (C/EBPα) was also assessed. HDF feeding caused a significant induction of C/EBPα (+30%, *vs* Control) and downregulation of FOXA1 (-27%). Quercetin supplementation was able to counteract this gene deregulation (FAT/CD36: -31%, FABP1: +51%, C/EBPα: -15%, and FOXA1: +40%, *vs* HFD group) (Fig. 2A).

Quercetin modulates HFD-induced dysbiosis in mice with HFD-induced NAFLD

Regarding to metagenomic analysis to determine the effect of HFD and quercetin on intestinal microbiota balance, given the characteristics of this study, the results obtained in the four experimental groups were separately considered (Control, ControlQ, HFD and HFDQ).

A total of 3,192,269 reads were obtained from the caecal samples through pyrosequencing analysis. Most of the identified reads from the caecal content of mice were classified within three phyla. *Firmicutes* phylum was predominant, representing 42% of 16S rRNA gene sequences, followed by *Bacteroidetes* (25%) and *Proteobacteria* (25%). These three phyla represented more than 90% of the sequences analyzed. Figure 3A shows the relative bacterial composition at the phylum level for each group. The relative abundance of *Firmicutes* and *Proteobacteria* phyla was significantly higher in HFD groups compared to the control groups. Nevertheless, quercetin supplementation was found to reduce significantly relative percentage of *Proteobacteria* phylum in HFD-fed mice, being similar to the control group with and without quercetin. However, changes in relative percentage of *Firmicutes* phylum associated with quercetin supplementation were not detected. There were also changes in the relative abundance of *Bacteroidetes* phylum. The mean relative abundance of this bacterial phylum in HFD group was reduced significantly compared to the control group with and without quercetin. Quercetin supplementation was found to considerably modify relative percentage of *Bacteroidetes* when compared to HFD-fed mice. Moreover, the ratio *Firmicutes*/*Bacteroidetes* was significantly different between control and HFD groups. Supplementation with quercetin in HFD-fed mice decreased significantly this ratio in relation to HFD group (Fig. 3B).

Comparison of the bacterial communities at phylum level using Principal Coordinates Analysis (PCoA) based on Morisita-Horn index was performed. The first axis score plot (10.63%) revealed a clear separation of bacterial communities according to the diet with or without quercetin supplementation (Fig. 3C).

At the class level, changes were detected comparing microbiota composition between control and HFD group, independently of quercetin. *Clostridia*, *Bacilli* (both classified

within the *Firmicutes* phylum) and *Deltaproteobacteria* (*Proteobacteria* phylum), were considerably increased in mice fed with HFD. On the contrary, *Bacteroidia* (*Bacteroidetes* phylum), *Erysipelotrichi* (*Firmicutes* phylum) and *Betaproteobacteria* (*Proteobacteria* phylum) were significantly reduced in HFD group in comparison to the control group. Quercetin supplementation in mice fed with HFD was found to considerably modify the number of reads of *Deltaproteobacteria*, *Bacteroidia*, *Erysipelotrichi* and *Betaproteobacteria* approaching to the control group in all cases ($p<0.05$) (data not shown).

We identified 420 different genera of known bacteria in caecal content. Most of the sequences belonged to the genera *Desulfovibrio*, *Blautia*, *Oscillospira*, *Akkermansia*, *Flavobacterium*, *Parabacteroides* and *Ruminococcus*. As shown in Fig. 4A, *Desulfovibrio*, *Blautia*, *Oscillospira* and *Lactobacillus* revealed a higher detection in mice fed with HFD group in comparison to the control group. Furthermore, quercetin supplementation in HFD-fed mice reduced significantly the detection of *Desulfovibrio*, showing similar values to the control group. Interestingly, changes related to quercetin treatment were also showed in *Helicobacter* genus. The dramatically increased detection of this genus in mice fed with HFD was significantly reduced with the oral supplementation with quercetin. Also, quercetin-dependent *Helicobacter* genus reduction was observed in the control group (Fig. 4B). Some bacterial genera, such as *Parabacteroides* and *Alkaliphilus*, showed an opposite pattern, with a lower detection in mice fed with HFD in comparison to the control group. *Flavobacterium*, *Allobaculum*, and *Sutturella*, besides presenting a low detection in HFD group, quercetin supplementation in HFD significantly increased the relative abundance of these genera. In both cases, the differences were associated with diet and quercetin, respectively. In addition, *Akkermansia*, the unique bacteria belonging to *Verrucomicrobia* phylum,

showed a notable increase with quercetin supplementation in control group and in mice fed with HFD compared to non-supplemented groups. However, these differences were not statistically significant (Fig. 4C).

Beta diversity measurements were performed on the caecal content to determine whether there were differences in global bacterial composition among the four groups. A PCoA based on Morosita Horn Index was performed showing that the bacterial communities of mice fed with HFD clustered together according to the first axis (14.47%) based on the diet. Whereas, the communities of control group were dispersed along this axis. The second axis score plot (3.17%) suggested a possible cluster of bacterial communities of mice fed with HFD according to the presence of quercetin in the diet (supplemental Fig. S1).

We also performed qPCR analysis for total bacteria evaluation in each sample. Similar to the pyrosequencing analysis findings from caecal samples, qPCR results revealed diet-dependent differences in bacterial concentration. Thus, HFD-fed mice showed a lower concentration of the total bacteria in each sample in comparison to control groups. However, HFDQ-fed mice increased this concentration, with values higher than the control group (Fig. 3D). The Kruskall-Wallis Test showed that these differences between the four groups were significant according to the diet and supplementation with quercetin.

To determine the potential relationship between the spectrum of NAFLD severity in response to HFD and differences in gut microbiota composition, correlation analysis was performed. As shown in supplemental Fig. S2, NAS significantly and positively correlated with *Firmicutes/Bacteroidetes* ratio and negatively correlated with total bacteria concentration.

Quercetin reverses HFD-induced SCFAs production inhibition and related intestinal barrier dysfunction

SCFAs, mainly acetate, propionate and butyrate, are produced by the intestinal microbiota. It has been reported that an increase in SCFAs concentration improves the integrity of the intestinal barrier [24]. As shown in Figure 5A, in our *in vivo* model of NAFLD, we found that SCFAs production in HFD-fed mice was lower than in control mice (acetate: -32%; propionate: -21%; butyrate: -29%, *vs* Control). Quercetin restores the low production of SCFAs induced by HFD (acetate: +34%; propionate: +27%; butyrate: +21%, *vs* HFD). These results correlated with the expression levels of intestinal tight-junction proteins claudin 1 and occludin and with intestinal phosphatase alkaline, significantly decreased in HFD-fed mice (claudin 1: -59%, occludin: -23%, and IAP: -41%) in comparison with control group. Quercetin supplementation restored the gut barrier function (claudin 1: +144%, occludin: +37%, and IAP: +40%; *vs* HFD) (Fig. 5B).

Quercetin counteracts HFD-induced endotoxemia, gut-liver axis activation and subsequent proinflammatory response induction in mice with HFD-induced NAFLD

Proven the imbalance of gut microbiota caused by the HFD in mice, dysbiosis-related bacterial lipopolysaccharide translocation and ethanol overproduction were determined. In our study, HFD-fed mice showed a significant increase in plasma LPS and ethanol levels (+73% and +34%, respectively, *vs* Control), which was reverted by quercetin treatment (-35% and -22%, respectively, *vs* HFD) (Fig. 6A). It is worthy of mention that HFD-induced endotoxemia was accompanied by a marked upregulation of hepatic TLR-4 gene expression (mRNA: +1416%, protein: +162%, *vs* Control). Quercetin

supplementation lowered TLR-4 mRNA and protein levels by about -67% and -42%, respectively, compared to HFD-fed mice (Fig. 6B).

Given the existence of endotoxemia and a concomitant overexpression of TLR-4 induced by HFD feeding, we analyzed the subsequent hepatic NF-κB signaling pathway activation. Since NF-κB activation is usually mediated by its nuclear translocation, we examined the effect of high fat diet on the cytosolic and nuclear NF-κB p65 subunit distribution by western blot. Fig. 6C showed the existence of NF-κB activation in HFD-fed mice, as evidenced by the increased presence of the p65 subunit in the nucleus (+112%, *vs* Control) instead of its cytosolic localization (-33%, *vs* control mice). Quercetin treatment was able to suppress HFD-induced NF-κB activation, as indicated by the permanence of p65 in the cytosolic localization (+24%, *vs* HFD), by means of the blockage of its nuclear translocation (-47%, *vs* HFD) (Fig. 6C).

To investigate the contribution of NF-κB-mediated proinflammatory response to the systemic inflammation associated to obesity and NAFLD, we studied the hepatic gene expression of cytokines tumor necrosis factor (TNF)-α and IL-6 in our HFD-based model. After 16 weeks of HFD feeding, we observed that diet caused a significant upregulation of TNF-α and IL-6 gene expression (+229% and +77%, respectively) that was effectively blocked by quercetin (-64% and -43%, respectively) (Fig. 6D). In this regard, we observed that HFD feeding induced an increase in plasma proinflammatory cytokine IL-6 in comparison with control mice (+268%) whereas quercetin supplementation partially attenuated hepatic plasma IL-6 release (-25%, *vs* HFD) (Table 3).

Quercetin inhibits hepatic NLRP3 inflammasome and its downstream pathway activation in mice with HFD-induced NAFLD

In order to investigate the participation of inflammasome initiation response modulation in the protective effect of quercetin on NAFLD progression and development, we analyzed hepatic expression levels of NLRP3 inflammasome components. As shown in Fig. 7A, high fat diet significantly increased gene expression of NLRP3 and caspase 1 activation (mRNA, NLRP3: +27%, caspase 1: +92%; protein, NLRP3: +37%, and active caspase 1: +64%) in comparison with control diet. Quercetin supplementation successfully restored hepatic NLRP3 inflammasome components gene expression and activation to control values (mRNA, NLRP3: -32% and caspase 1: -47%; protein, NLRP3: -48% and active caspase 1: -40%) (Fig. 7A).

Quercetin inhibits HFD-related endoplasmic reticulum stress pathway induction in mice with HFD-induced NAFLD

To examine the contribution of the activation of the unfolded protein response (UPR) related to endoplasmic reticulum (ER) stress in the development of NAFLD in our HFD-based model we determined the ER stress markers GRP78 and CHOP. As shown in Fig. 7B, HFD feeding increased gene expression of GRP78 and CHOP (mRNA, GRP78: +47% and CHOP: +63%; protein, GRP78: +88% and CHOP: +101%, *vs* Control). Quercetin treatment significantly inhibited HFD-induced overexpression of ER stress markers (mRNA, GRP78: -34%, and CHOP: -42%; protein, GRP78: -37% and CHOP: -21%, *vs* HFD-fed mice).

Discussion

There is growing evidence supporting the causative role of gut microbiota in NAFLD development and progression, by a mechanism involving obesity induction, endogenous ethanol production, inflammatory response activation and metabolism deregulation, among others [8, 25]. In this respect, in our animal model of NAFLD a relationship between dysbiosis mediated-inflammatory response and lipid metabolism alteration is involved in the development of obesity-associated fatty liver disease. Also, we describe for the first time that the protective effect of quercetin on NAFLD is mediated by the modulation of intestinal microbiota imbalance and related gut-liver axis activation, counteracting inflammasome initiation response as well as reticulum stress pathway induction, in an integrative mechanism involving its anti-inflammatory, antioxidant and prebiotic capacities.

Feeding animals with high-fat diet induce obesity, metabolic syndrome and its hepatic manifestation, NAFLD, mimicking the metabollicaly obese phenotype of Western countries. In our study, HFD feeding induced body weight gain and visceral obesity, hyperglycemia, insulin resistance and dyslipidemia. It has been described that quercetin possesses anti-insulin resistance properties, ameliorating insulin sensitivity and glucose intolerance [26, 27]. Our results corroborate the modulatory capacity of quercetin on glucose homeostasis through the improvement of glucose tolerance and insulin sensitivity despite the high fat diet intake, as previously described in an *in vivo* model of obesity in rats [16]. Moreover, the protective role of quercetin on glucose homeostasis was accompanied by a limited but significant reduction of body weight gain independent of food intake.

Hepatic steatosis was the principal histopathological finding, as observed in other studies in mice fed a high-fat diet [28, 29]. Oral supplementation with quercetin in

HFD-fed mice counteracts increased liver weight by reducing liver steatosis derived from a disminished plasma dyslipidemia and hepatic triglyceride accumulation, supporting the protective effect of quercetin on metabolic biomarkers in experimentally induced NAFLD [5, 30, 31].

Previous research has already shown that quercetin prevents HFD-induced dyslipidemia and steatosis by means of its modulatory effect on hepatic gene expression related to lipid metabolism [32, 33]. In this regard, our findings indicate that HFD-induced steatosis results mainly from increased *de novo* lipogenesis and lipid uptake. Thus, in the current study LXRα and its downstream lipogenic genes were overexpressed in HFD-fed mice. LXRα plays a role as a contributing factor for NAFLD-related steatosis development by enhancing lipogenesis in *in vivo* and *in vitro* models and in the liver of patients [5, 34]. This transcription factor increases fatty acid synthesis by either upregulating SREBP-1c or directly binding to the promoters of lipogenic genes, including fatty acid synthase [34]. In the present study, quercetin supplementation in HFD-fed mice was able to counteract lipogenic genes upregulation, corroborating the capacity of this flavonol to modulate lipogenesis at the transcriptional level in *in vivo* and *in vitro* models of NAFLD [5, 31].

In spite of the role of *de novo* lipogenesis deregulation, fatty acid uptake seems to play a key implication in the pathogenesis of NAFLD [5, 22, 32, 35]. In the present study, quercetin treatment modulated the impaired gene expression of several fatty acid uptake- and trafficking-related proteins. It has already been reported the downregulation of fatty acid binding protein 1 in *in vivo* models and patients with NAFLD, as corroborated in the present study. Additionally, FABP1 repression was associated to the impaired expression of transcription factors FOXA1 and C/EBPα, contributing to exacerbate lipotoxicity and lipid accumulation in NAFLD [35]. Our results also confirm

previous observations showing that quercetin treatment attenuated FABP1 downregulation through the modulation of their major regulatory transcription factors in different models of NAFLD [5]. Moreover, findings support the capacity of quercetin to reduce FAT/CD36 upregulation associated with insulin resistance and steatosis, as previously observed in several nutritional models of NAFLD [5, 32].

On the other hand, NAFLD may be indirectly dependent on pathways associated with microbiota-induced obesity through inflammation mediated by the immune system [10, 36, 37]. Likewise, the gut microbiota composition could also contribute to the development of NAFLD independently of obesity [29]. It has been previously reported that feeding a high fat diet caused gut microbiota imbalance as a mechanism involved in obese-related NAFLD development, justifying the adequacy of the current study [38, 39]. As expected, in our murine model of NAFLD metagenomic studies revealed differences at phylum, class and genus levels between HFD-fed mice and controls, leading to dysbiosis. As previously described, HFD-induced dysbiosis was characterized by an increase in Gram-negative bacteria and, most important, by a general decrease of total bacteria concentration [40]. In turn, it has been described that differences in gut microbial composition can determine response to HFD in mice [29, 41], which would explain the wide spectrum of NAFLD observed in our study in accordance with the individual metabolic phenotype, as corroborated by results obtained from correlation analysis.

Previous *in vitro* and *in vivo* research indicated that flavonols have a prebiotic-like effect, playing a role on intestinal mucosa inflammation and permeability [13, 15, 16]. In turn, polyphenols modulate the intestinal microbiota and indirectly interfere with their own bioavailability [14, 15]. Thereby, quercetin has low bioavailability and, as several flavonoids, it is target of the gut microbial ecosystem [16]. In the current study,

quercetin supplementation in HFD-fed mice caused a great impact on gut microbiota composition at different taxonomic levels, counteracting the gut microbiota dysbiosis. Thus, quercetin reduced the increased *Firmicutes/Bacteroidetes* ratio as well as the enhanced Gram-negative *Proteobacteria* phylum in HFD-fed mice and increased the concentration of total bacteria. At the class level, HFD-related *Clostridia*, *Bacilli* and *Deltraproteobacteria* increase and *Bacteroidi*a, *Erysipelotrichi* and *Betaproteobacteria* reduction reverted to control values when supplemented with quercetin. These results support the prebiotic capacity of this flavonol reported in a previous model of obesity in rats [16].

We also identified genera differently represented in HFD-fed mice, which detection values tended to be similar to control groups when quercetin was added. Recent studies show that *Akkermansia muciniphila* inversely correlates with obesity in rodents and patients [42, 43]. In this regard, we observed a HFD-related reduction in *Akkermansia* genus detection, which raised with quercetin treatment, as previously shown in association with obesity [16]. Similarly, betacyanins obtained from Red pitaya (*Hylocereus polyrhizus*) fruit also induced an increase in the relative abundance of *Akkermansia* at the genus level in HFD-fed mice [44]. This result suggests that quercetin could reduce body weight gain, at least in part, by restoring gut microbiota balance. Moreover, we describe for the first time the association between high fat diet-induced NAFLD and enhanced *Helicobacter* genus detection. Even though is a controversial issue [45, 46], it has been suggested the role of *Helicobacter pilory* as a contributing factor in the progression of NAFLD [47-49], considering its eradication as effective preventive or treatment measures [50, 51]. Interestingly, *Helicobacter* genus was dramatically reduced by quercetin treatment in our model of NAFLD, corroborating its anti-*Helicobacter* activity observed in *in vitro* and *in vivo* models of infection [52,

53], and supporting therapeutic potential of quercetin for prevention of the spectrum of non-alcoholic fatty liver diseases.

Dysbiosis-related bacterial endotoxins, such as lipopolysaccharide and ethanol, play a key role in the pathogenesis of NAFLD [10, 54]. Specific pattern recognition receptors (PRRs) participate in the microbial recognition process of highly conserved microbial signature molecules called pathogen-associated molecular patterns (PAMPs) and the endogenous danger-associated molecular patterns (DAMPs). The PRRs include toll-like receptors and nucleotide-binding and oligomerization domain (NOD)-like receptors [55]. The LPS of Gram-negative bacterial cell walls is the major PAMP, and a natural TLR ligand [56]. Some authors have reported that the activation of TLR-4 is involved in the development and progression of NAFLD [4, 10]. In our study, HFD-induced disruption of intestinal bacterial balance was accompanied by ethanol overproduction and lipopolysaccharide translocation associated with an impaired intestinal SCFAs production and an altered barrier function. In fact, in HFD-fed mice bacterial product activation induced gut-liver axis alteration through TLR-4 overexpression and subsequent nuclear factor kappa B signaling pathway activation, leading to induction of a proinflammatory response mediated by TNF-α and IL-6. These results corroborate that the activation of TLR-4 and its downstream pathway plays a key role on the gut-liver axis alteration associated to dysbiosis and related NAFLD development [57, 58]. In the current research, beneficial effect on NAFLD by quercetin in HFD-fed mice is mediated by modulation of gut microbiota balance and subsequent reduction of plasma LPS and ethanol contents, restoring SCFAs production and intestinal barrier integrity. These findings were associated with a marked inhibition of HFD-induced TLR-4 expression at transcriptional level and the modulation of TLR-4-NF-κB signaling pathway activation by quercetin, and a downregulation of TNF-α and IL-6 gene

expression, confirming its well-known anti-inflammatory capacity [5, 26, 59, 60]. TNF-α and IL-6 play a key role in glucose homeostasis impairment associated with HFD [61], suggesting that proinflammatory cytokines blockage by quercetin contributes to its anti-insulin resistance properties.

A common denominator in the pathogenesis of NAFLD is CYP2E1-dependent oxidative stress, as a key mechanism responsible for liver damage and disease progression [62]. In our study, quercetin protects liver against NAFLD by reducing CYP2E1 overexpression and subsequent oxidative stress, in agreement with results obtained in a similar *in vivo* model [63]. Also, results obtained confirm the capacity of quercetin to reduce lipid peroxidation described in several models of NAFLD [5, 26, 30]. It has been reported the central role of lipotoxicity in the recruitment of innate immunity involving TLR [64]. In our study, higher degree of lipoperoxidation in HFD-fed mice was associated with TLR-4-mediated NF-κB activation and subsequent inflammatory gene overexpression. It has been previously suggested that quercetin negatively regulates TLR-4 signaling induced by lipopolysaccharide through Toll-interacting protein expression, a negative regulator of TLR signaling [65]. In our model of NAFLD, quercetin treatment attenuated lipoperoxidation-dependent TLR-4 pathway activation, as an alternative mechanism contributing to the modulatory capacity of this flavonol on gut-liver axis pathway.

Intestinal microbiota composition modulates glucose homeostasis and hepatic lipid metabolism, contributing to NAFLD development as an environmental factor [29, 66]. Thus, gut microbiota is involved in hepatic lipid metabolism gene regulation [10]. However, detailed mechanisms involving gut microbiota-mediated lipid metabolism gene expression modulation in the pathogenesis of NAFLD remain unclear. It has been demonstrated that bacterial LPS enhances hepatic fatty acid synthesis, while inhibiting

fatty acid oxidation in liver by reducing FABP gene expression [67]. Thereby, TLR-4 expression upregulation correlated with increased LPS and fatty acids, and associated with induced *de novo* lipogenesis in NAFLD patients [68]. Thus, TLR-4 plays a critical role in glucose and lipid metabolism and, in turn, free fatty acids have been reported as agonists for TLR-4 [69, 70], inducing activation of inflammatory transcription factors as NF-κB [69]. In the present research, overexpression of TLR-4 and activation of its downstream molecules in HFD-fed mice was associated with insulin resistance and lipid metabolism gene deregulation, supporting the role of gut-liver axis-mediated TLR signaling activation on the development of steatosis in the pathogenesis of NAFLD. Recently, we have described the protective effect of quercetin on lipid metabolism expression deregulation through the modulation of key pathways as PI3K/AKT signaling [5]. Likewise, the capacity of quercetin to downregulate dysbiosis-related TLR-4 signaling pathway activation could contribute to counteract gene expression deregulation associated to lipid metabolism-related pathways alteration implicated in NAFLD development.

Hepatic free fatty acid content was increased in HFD-fed mice, which could serve as substrate for lipotoxic metabolites formation involved in liver injury leading to NAFLD [71]. The effects of these lipotoxic lipid species on NAFLD development and progression may be exerted by stimulating oxidative stress and TLR-mediated proinflammatory signalling via NF-κB or by inducing endoplasmic reticulum stress [64, 72]. ER stress is one of the most important factors for disease progression in NAFLD [4]. Thus, reticulum stress disturbs hepatic lipid metabolism by deregulation of lipogenic genes, promotes insulin resistance, and activates several proinflammatory pathways as NF-κB [73, 74]. It has been described that the inflammatory response mediates the effect of dysbiosis and endotoxemia in ER stress development [75].

Moreover, several studies have described a relationship between CYP2E1 and ER stress [76, 77], contributing to NAFLD development [78]. It has already been reported that HFD feeding induced the activation of the unfolded protein response (UPR) related to reticulum stress [79]. In fact, in the present study HFD increased the gene expression of the ER stress markers GRP78 and CHOP, similarly to findings shown in patients whith NAFLD [80]. Quercetin supplementation to HFD-fed mice reverted gene expression deregulation associated to this stress pathway. The beneficial effect of quercetin on reticulum stress could be exerted by a complex mechanism underlying its modulatory effect on dysbiosis-mediated gut-liver axis activation and also by counteracting FFA and CYP2E1-dependent lipotoxicity as a result of its antioxidant activity, as previouly suggested [81]. The blockage of reticulum stress by quercetin could be relevant in the progression of steatosis to steatohepatitis, given its central role in the pathogenesis of NAFLD [80].

Inflammasomes are multiprotein complexes composed of a NOD-like receptor family, NLRP3, apoptosis-associated speck-like protein containing a CARD (ASC) and procaspase 1 that act as PAMP and DAMP sensors [4]. The NLRP3 binding to ASC causes caspase-1 activation, driving the inflammatory response [82]. The ligands and triggers of inflammasome initiation response in NAFLD are only partially understood. However, it has been recently reported that both activation of dysbiosis-induced TLR-NF-κB signaling pathway and oxidative stress-related lipotoxicity are involved in inflammasome response, which regulate the development and progression of NAFLD [9, 10, 83]. We observed an overexpression of hepatic inflammasome component NLRP3 and the subsequent activation of caspase-1, which could be associated with disease progression as shown in patients with NAFLD [84]. Also, a gender specific inflammasome activation has been reported in male mice fed a high-fat diet as NAFLD

model [85]. As expected, quercetin significantly inhibited sobreexpression of NLRP3 inflammasome and its downstream pathway activation because of its proven capacity to counteract dysbiosis-related TLR induction in addition to its well-known antioxidant properties, supporting previous results obtained in an *in vivo* model of diabetes [86]. Furthermore, it has been found that oxidative stress-mediated NLRP3 inflammasome activation also promoted lipid accumulation by deregulation of lipid metabolism-related genes expression in a high-fat diet model of NAFLD [87]. Consequently, a similar mechanism involving inflammasome initiation response blockage by quercetin may also underlie its modulatory effect on hepatic gene expression related to lipid metabolism alteration, reinforcing the role of this flavonol as a potential therapeutic strategy for preventing NAFLD development and progression.

Conclusions

Our results suggest that quercetin exerts its protective effect on HFD-induced NAFLD development by means of integrative responses involving its antioxidant, anti-inflammatory and prebiotic capacities. Thus, the modulatory activity of quercetin is mediated by intestinal microbiota dysbiosis, related gut-liver axis activation and lipotoxicity blockage, and subsequent inhibition of inflammasome response and reticulum stress pathway activation. Finally, these modulatory effects displayed by quercetin counteract lipid metabolism gene expression deregulation implicated in the development and progression of obesity-associated fatty liver disease (Fig. 8). However, further investigations to establish the precise molecular mechanisms implicated are necessary.

Acknowledgements

This work was supported by grants to Javier González-Gallego and Sonia Sánchez Campos from Ministerio de Economía y Competitividad/FEDER (BFU2013-48141-R) and Junta de Castilla y León (LE135U13 and BIO/LE02/15), LE063U16 (Junta de Castilla y León y Fondo Europeo de Desarrollo Regional (FEDER)) and Ramiro Jover from Fondo de Investigación Sanitaria (FIS), Instituto de Salud Carlos III (ISCIII-FEDER PI 13/01470). María V. García-Mediavilla was supported by CIBERehd contracts. CIBERehd is funded by the Instituto de Salud Carlos III, Spain.

The authors declare no conflict of interest.

References

[1] Vernon, G.; Baranova, A.; Younossi, Z. M. Systematic review: The epidemiology and natural history of non-alcoholic fatty liver disease and non-alcoholic steatohepatitis in adults. *Aliment. Pharmacol. Ther.* 34:274-285; 2011. doi: 10.1111/j.1365-2036.2011.04724.x.

[2] Machado, M.; Cortez-Pinto, H. Non-alcoholic steatohepatitis and metabolic syndrome. *Curr. Opin. Clin. Nutr. Metab. Care* 9:637-642; 2006. doi: 10.1097/01.mco.0000241677.40170.17.

[3] Tiniakos, D. G.; Vos, M. B.; Brunt, E. M. Nonalcoholic fatty liver disease: Pathology and pathogenesis. *Annu. Rev. Pathol.* 5:145-171; 2010. doi: 10.1146/annurev-pathol-121808-102132.

[4] Takaki, A.; Kawai, D.; Yamamoto, K. Multiple hits, including oxidative stress, as pathogenesis and treatment target in non-alcoholic steatohepatitis (NASH). *Int. J. Mol. Sci.* 14:20704-20728; 2013. doi: 10.3390/ijms141020704.

[5] Pisonero-Vaquero, S.; Martinez-Ferreras, A.; Garcia-Mediavilla, M. V.; Martinez-Florez, S.; Fernandez, A.; Benet, M.; Olcoz, J. L.; Jover, R.; Gonzalez-Gallego, J.; Sanchez-Campos, S. Quercetin ameliorates dysregulation of lipid metabolism genes via the PI3K/AKT pathway in a diet-induced mouse model of nonalcoholic fatty liver disease. *Mol. Nutr. Food Res.* 59:879-893; 2015. doi: 10.1002/mnfr.201400913.

[6] Buzzetti, E.; Pinzani, M.; Tsochatzis, E. A. The multiple-hit pathogenesis of non-alcoholic fatty liver disease (NAFLD). *Metabolism* 65:1038-1048; 2016. doi: 10.1016/j.metabol.2015.12.012.

[7] Usami, M.; Miyoshi, M.; Yamashita, H. Gut microbiota and host metabolism in liver cirrhosis. *World J. Gastroenterol.* 21:11597-11608; 2015. doi: 10.3748/wjg.v21.i41.11597.

[8] Abu-Shanab, A.; Quigley, E. M. The role of the gut microbiota in nonalcoholic fatty liver disease. *Nat. Rev. Gastroenterol. Hepatol.* 7:691-701; 2010. doi: 10.1038/nrgastro.2010.172.

[9] Henao-Mejia, J.; Elinav, E.; Jin, C.; Hao, L.; Mehal, W. Z.; Strowig, T.; Thaiss, C. A.; Kau, A. L.; Eisenbarth, S. C.; Jurczak, M. J.; Camporez, J. P.; Shulman, G. I.; Gordon, J. I.; Hoffman, H. M.; Flavell, R. A. Inflammasome-mediated dysbiosis regulates progression of NAFLD and obesity. *Nature* 482:179-185; 2012. doi: 10.1038/nature10809.

[10] Aron-Wisnewsky, J.; Gaborit, B.; Dutour, A.; Clement, K. Gut microbiota and non-alcoholic fatty liver disease: New insights. *Clin. Microbiol. Infect.* 19:338-348; 2013. doi: 10.1111/1469-0691.12140.

[11] Boursier, J.; Mueller, O.; Barret, M.; Machado, M.; Fizanne, L.; Araujo-Perez, F.; Guy, C. D.; Seed, P. C.; Rawls, J. F.; David, L. A.; Hunault, G.; Oberti, F.; Cales,

P.; Diehl, A. M. The severity of nonalcoholic fatty liver disease is associated with gut dysbiosis and shift in the metabolic function of the gut microbiota. *Hepatology* 63:764-775; 2016. doi: 10.1002/hep.28356.

[12] Lambert, J. E.; Parnell, J. A.; Eksteen, B.; Raman, M.; Bomhof, M. R.; Rioux, K. P.; Madsen, K. L.; Reimer, R. A. Gut microbiota manipulation with prebiotics in patients with non-alcoholic fatty liver disease: A randomized controlled trial protocol. *BMC Gastroenterol.* 15:169-015-0400-5; 2015. doi: 10.1186/s12876-015-0400-5.

[13] Kawabata, K.; Sugiyama, Y.; Sakano, T.; Ohigashi, H. Flavonols enhanced production of anti-inflammatory substance(s) by bifidobacterium adolescentis: Prebiotic actions of galangin, quercetin, and fisetin. *Biofactors* 39:422-429; 2013. doi: 10.1002/biof.1081.

[14] Cardona, F.; Andres-Lacueva, C.; Tulipani, S.; Tinahones, F. J.; Queipo-Ortuno, M. I. Benefits of polyphenols on gut microbiota and implications in human health. *J. Nutr. Biochem.* 24:1415-1422; 2013. doi: 10.1016/j.jnutbio.2013.05.001.

[15] Duda-Chodak, A.; Tarko, T.; Satora, P.; Sroka, P. Interaction of dietary compounds, especially polyphenols, with the intestinal microbiota: A review. *Eur. J. Nutr.* 54:325-341; 2015. doi: 10.1007/s00394-015-0852-y.

[16] Etxeberria, U.; Arias, N.; Boque, N.; Macarulla, M. T.; Portillo, M. P.; Martinez, J. A.; Milagro, F. I. Reshaping faecal gut microbiota composition by the intake of trans-resveratrol and quercetin in high-fat sucrose diet-fed rats. *J. Nutr. Biochem.* 26:651-660; 2015. doi: 10.1016/j.jnutbio.2015.01.002.

[17] Kleiner, D. E.; Brunt, E. M.; Van Natta, M.; Behling, C.; Contos, M. J.; Cummings, O. W.; Ferrell, L. D.; Liu, Y. C.; Torbenson, M. S.; Unalp-Arida, A.; Yeh, M.; McCullough, A. J.; Sanyal, A. J.; Nonalcoholic Steatohepatitis Clinical

Research Network. Design and validation of a histological scoring system for nonalcoholic fatty liver disease. *Hepatology* 41:1313-1321; 2005. doi: 10.1002/hep.20701.

[18] Whelan, K.; Judd, PA.; Tuohy, KM.; Gibson, GR.; Preedy, VR.; Taylor, MA. Fecal microbiota in patients receiving enteral feeding are highly variable and may be altered in those who develop diarrhea. Am J Clin Nutr. 89 Suppl 1:240–247; 2009. doi: 10.3945/ajcn.2008.26219.

[19] Herlemann, D. P.; Labrenz, M.; Jurgens, K.; Bertilsson, S.; Waniek, J. J.; Andersson, A. F. Transitions in bacterial communities along the 2000 km salinity gradient of the baltic sea. *Isme J.* 5:1571-1579; 2011. doi: 10.1038/ismej.2011.41.

[20] Illumina. 16S metagenomics app 15055860 A ed2014. available from: Https://Support.illumina.com/content/dam/illumina-support/documents/documentation/software_documentation/basespace/16s-metagenomics-user-guide-15055860-a.pdf.

[21] Oksanen, J.; Blanchet, F. G.; Kindt, R.; Legendre, P.; Minchin, P. R.; O'Hara, R. B.; Simpson, G. L. :. S., P.; Stevens, M. H. H.; Wagner, H. H. Vegan: Community ecology R package, v2. 0-10.

[22] Miquilena-Colina, M. E.; Lima-Cabello, E.; Sanchez-Campos, S.; Garcia-Mediavilla, M. V.; Fernandez-Bermejo, M.; Lozano-Rodriguez, T.; Vargas-Castrillon, J.; Buque, X.; Ochoa, B.; Aspichueta, P.; Gonzalez-Gallego, J.; Garcia-Monzon, C. Hepatic fatty acid translocase CD36 upregulation is associated with insulin resistance, hyperinsulinaemia and increased steatosis in non-alcoholic steatohepatitis and chronic hepatitis C. *Gut* 60:1394-1402; 2011. doi: 10.1136/gut.2010.222844.

[23] Chao, J.; Huo, T. I.; Cheng, H. Y.; Tsai, J. C.; Liao, J. W.; Lee, M. S.; Qin, X. M.; Hsieh, M. T.; Pao, L. H.; Peng, W. H. Gallic acid ameliorated impaired glucose and lipid homeostasis in high fat diet-induced NAFLD mice. *PLoS One* 9:e96969; 2014. doi: 10.1371/journal.pone.0096969.

[24] Suzuki T. Regulation of intestinal epithelial permeability by tight junctions. *Cell Mol Life Sci* 70: 631-659; 2013. doi: 10.1007/s00018-012-1070-x.

[25] Gkolfakis, P.; Dimitriadis, G.; Triantafyllou, K. Gut microbiota and non-alcoholic fatty liver disease. *Hepatobiliary. Pancreat. Dis. Int.* 14:572-581; 2015. doi: 10.1016/S1499-3872(15)60026-1.

[26] Vidyashankar, S.; Sandeep Varma, R.; Patki, P. S. Quercetin ameliorate insulin resistance and up-regulates cellular antioxidants during oleic acid induced hepatic steatosis in HepG2 cells. *Toxicol. in. Vitro.* 27:945-953; 2013. doi: 10.1016/j.tiv.2013.01.014.

[27] Dong, J.; Zhang, X.; Zhang, L.; Bian, H. X.; Xu, N.; Bao, B.; Liu, J. Quercetin reduces obesity-associated ATM infiltration and inflammation in mice: A mechanism including AMPKalpha1/SIRT1. *J. Lipid Res.* 55:363-374; 2014. doi: 10.1194/jlr.M038786.

[28] Nishikawa, S.; Yasoshima, A.; Doi, K.; Nakayama, H.; Uetsuka, K. Involvement of sex, strain and age factors in high fat diet-induced obesity in C57BL/6J and BALB/cA mice. *Exp. Anim.* 56:263-272; 2007. doi: 10.1538/expanim.56.263.

[29] Le Roy, T.; Llopis, M.; Lepage, P.; Bruneau, A.; Rabot, S.; Bevilacqua, C.; Martin, P.; Philippe, C.; Walker, F.; Bado, A.; Perlemuter, G.; Cassard-Doulcier, A. M.; Gerard, P. Intestinal microbiota determines development of non-alcoholic fatty liver disease in mice. *Gut* 62:1787-1794; 2013. doi: 10.1136/gutjnl-2012-303816.

[30] Surapaneni, K. M.; Jainu, M. Pioglitazone, quercetin and hydroxy citric acid effect on hepatic biomarkers in non alcoholic steatohepatitis. *Pharmacognosy Res.* 6:153-162; 2014. doi: 10.4103/0974-8490.129037.

[31] Wang, L. L.; Zhang, Z. C.; Hassan, W.; Li, Y.; Liu, J.; Shang, J. Amelioration of free fatty acid-induced fatty liver by quercetin-3-O-beta-D-glucuronide through modulation of peroxisome proliferator-activated receptor-alpha/sterol regulatory element-binding protein-1c signaling. *Hepatol. Res.* 46:225-238; 2016. doi: 10.1111/hepr.12557.

[32] Jung, C. H.; Cho, I.; Ahn, J.; Jeon, T. I.; Ha, T. Y. Quercetin reduces high-fat diet-induced fat accumulation in the liver by regulating lipid metabolism genes. *Phytother. Res.* 27:139-143; 2013. doi: 10.1002/ptr.4687.

[33] Monika, P.; Geetha, A. The modulating effect of persea americana fruit extract on the level of expression of fatty acid synthase complex, lipoprotein lipase, fibroblast growth factor-21 and leptin--A biochemical study in rats subjected to experimental hyperlipidemia and obesity. *Phytomedicine* 22:939-945; 2015. doi: 10.1016/j.phymed.2015.07.001.

[34] Lima-Cabello, E.; Garcia-Mediavilla, M. V.; Miquilena-Colina, M. E.; Vargas-Castrillon, J.; Lozano-Rodriguez, T.; Fernandez-Bermejo, M.; Olcoz, J. L.; Gonzalez-Gallego, J.; Garcia-Monzon, C.; Sanchez-Campos, S. Enhanced expression of pro-inflammatory mediators and liver X-receptor-regulated lipogenic genes in non-alcoholic fatty liver disease and hepatitis C. *Clin. Sci. (Lond)* 120:239-250; 2011. doi: 10.1042/CS20100387.

[35] Guzman, C.; Benet, M.; Pisonero-Vaquero, S.; Moya, M.; Garcia-Mediavilla, M. V.; Martinez-Chantar, M. L.; Gonzalez-Gallego, J.; Castell, J. V.; Sanchez-Campos, S.; Jover, R. The human liver fatty acid binding protein (FABP1) gene is

activated by FOXA1 and PPARalpha; and repressed by C/EBPalpha: Implications in FABP1 down-regulation in nonalcoholic fatty liver disease. *Biochim. Biophys. Acta* 1831:803-818; 2013. doi: 10.1016/j.bbalip.2012.12.014.

[36] Wood, N. J. Microbiota: Dysbiosis driven by inflammasome deficiency exacerbates hepatic steatosis and governs rate of NAFLD progression. *Nat. Rev. Gastroenterol. Hepatol.* 9:123; 2012. doi: 10.1038/nrgastro.2012.21.

[37] Bieghs, V.; Trautwein, C. Innate immune signaling and gut-liver interactions in non-alcoholic fatty liver disease. *Hepatobiliary. Surg. Nutr.* 3:377-385; 2014. doi: 10.3978/j.issn.2304-3881.2014.12.04.

[38] Mei, L.; Tang, Y.; Li, M.; Yang, P.; Liu, Z.; Yuan, J.; Zheng, P. Co-administration of cholesterol-lowering probiotics and anthraquinone from Cassia obtusifolia L. ameliorate non-alcoholic fatty liver. *PLoS One* 10:e0138078; 2015. doi: 10.1371/journal.pone.0138078.

[39] Tian, Y.; Wang, H.; Yuan, F.; Li, N.; Huang, Q.; He, L.; Wang, L.; Liu, Z. Perilla oil has similar protective effects of fish oil on high-fat diet-induced nonalcoholic fatty liver disease and gut dysbiosis. *Biomed. Res. Int.* 2016:9462571; 2016. doi: 10.1155/2016/9462571.

[40] De Minicis, S.; Rychlicki, C.; Agostinelli, L.; Saccomanno, S.; Candelaresi, C.; Trozzi, L.; Mingarelli, E.; Facinelli, B.; Magi, G.; Palmieri, C.; Marzioni, M.; Benedetti, A.; Svegliati-Baroni, G. Dysbiosis contributes to fibrogenesis in the course of chronic liver injury in mice. *Hepatology* 59:1738-1749; 2014. doi: 10.1002/hep.26695.

[41] Serino, M.; Luche, E.; Gres, S.; Baylac, A.; Berge, M.; Cenac, C.; Waget, A.; Klopp, P.; Iacovoni, J.; Klopp, C.; Mariette, J.; Bouchez, O.; Lluch, J.; Ouarne, F.; Monsan, P.; Valet, P.; Roques, C.; Amar, J.; Bouloumie, A.; Theodorou, V.;

Burcelin, R. Metabolic adaptation to a high-fat diet is associated with a change in the gut microbiota. *Gut* 61:543-553; 2012. doi: 10.1136/gutjnl-2011-301012.

[42] Everard, A.; Belzer, C.; Geurts, L.; Ouwerkerk, J. P.; Druart, C.; Bindels, L. B.; Guiot, Y.; Derrien, M.; Muccioli, G. G.; Delzenne, N. M.; de Vos, W. M.; Cani, P. D. Cross-talk between Akkermansia muciniphila and intestinal epithelium controls diet-induced obesity. *Proc. Natl. Acad. Sci. U. S. A.* 110:9066-9071; 2013. doi: 10.1073/pnas.1219451110.

[43] Miura, K.; Ohnishi, H. Role of gut microbiota and toll-like receptors in nonalcoholic fatty liver disease. *World J. Gastroenterol.* 20:7381-7391; 2014. doi: 10.3748/wjg.v20.i23.7381.

[44] Song, H.; Chu, Q.; Yan, F.; Yang, Y.; Han, W.; Zheng, X. Red pitaya betacyanins protects from diet-induced obesity, liver steatosis and insulin resistance in association with modulation of gut microbiota in mice. *J. Gastroenterol. Hepatol.* 2015. doi: 10.1111/jgh.13278.

[45] Okushin, K.; Takahashi, Y.; Yamamichi, N.; Shimamoto, T.; Enooku, K.; Fujinaga, H.; Tsutsumi, T.; Shintani, Y.; Sakaguchi, Y.; Ono, S.; Kodashima, S.; Fujishiro, M.; Moriya, K.; Yotsuyanagi, H.; Mitsushima, T.; Koike, K. Helicobacter pylori infection is not associated with fatty liver disease including non-alcoholic fatty liver disease: A large-scale cross-sectional study in Japan. *BMC Gastroenterol.* 15:25-015-0247-9; 2015. doi: 10.1186/s12876-015-0247-9.

[46] Baeg, M. K.; Yoon, S. K.; Ko, S. H.; Noh, Y. S.; Lee, I. S.; Choi, M. G. Helicobacter pylori infection is not associated with nonalcoholic fatty liver disease. *World J. Gastroenterol.* 22:2592-2600; 2016. doi: 10.3748/wjg.v22.i8.2592.

[47] Sumida, Y.; Kanemasa, K.; Imai, S.; Mori, K.; Tanaka, S.; Shimokobe, H.; Kitamura, Y.; Fukumoto, K.; Kakutani, A.; Ohno, T.; Taketani, H.; Seko, Y.;

Ishiba, H.; Hara, T.; Okajima, A.; Yamaguchi, K.; Moriguchi, M.; Mitsuyoshi, H.; Yasui, K.; Minami, M.; Itoh, Y. Helicobacter pylori infection might have a potential role in hepatocyte ballooning in nonalcoholic fatty liver disease. *J. Gastroenterol.* 50:996-1004; 2015. doi: 10.1007/s00535-015-1039-2.

[48] Waluga, M.; Kukla, M.; Zorniak, M.; Bacik, A.; Kotulski, R. From the stomach to other organs: Helicobacter pylori and the liver. *World J. Hepatol.* 7:2136-2146; 2015. doi: 10.4254/wjh.v7.i18.2136.

[49] Zhang, C.; Guo, L.; Qin, Y.; Li, G. Correlation between helicobacter pylori infection and polymorphism of adiponectin gene promoter-11391G/A, superoxide dismutase gene innonalcoholic fatty liver disease. *Zhong Nan Da Xue Xue Bao Yi Xue Ban* 41:359-366; 2016. doi: 10.11817/j.issn.1672-7347.2016.04.004.

[50] Jamali, R.; Mofid, A.; Vahedi, H.; Farzaneh, R.; Dowlatshahi, S. The effect of helicobacter pylori eradication on liver fat content in subjects with non-alcoholic fatty liver disease: A randomized open-label clinical trial. *Hepat Mon.* 13:e14679; 2013. doi: 10.5812/hepatmon.14679.

[51] Polyzos, S. A.; Kountouras, J.; Papatheodorou, A.; Patsiaoura, K.; Katsiki, E.; Zafeiriadou, E.; Zavos, C.; Anastasiadou, K.; Terpos, E. Helicobacter pylori infection in patients with nonalcoholic fatty liver disease. *Metabolism* 62:121-126; 2013. doi: 10.1016/j.metabol.2012.06.007.

[52] Gonzalez-Segovia, R.; Quintanar, J. L.; Salinas, E.; Ceballos-Salazar, R.; Aviles-Jimenez, F.; Torres-Lopez, J. Effect of the flavonoid quercetin on inflammation and lipid peroxidation induced by Helicobacter pylori in gastric mucosa of guinea pig. *J. Gastroenterol.* 43:441-447; 2008. doi: 10.1007/s00535-008-2184-7.

[53] Wang, Y. C. Medicinal plant activity on Helicobacter pylori related diseases. *World J. Gastroenterol.* 20:10368-10382; 2014. doi: 10.3748/wjg.v20.i30.10368.

[54] Imajo, K.; Yoneda, M.; Ogawa, Y.; Wada, K.; Nakajima, A. Microbiota and nonalcoholic steatohepatitis. *Semin. Immunopathol.* 36:115-132; 2014. doi: 10.1007/s00281-013-0404-6.

[55] Ganz, M.; Szabo, G. Immune and inflammatory pathways in NASH. *Hepatol. Int.*7 Suppl 2:771-781; 2013. doi: 10.1007/s12072-013-9468-6.

[56] Calabrese, V.; Cighetti, R.; Peri, F. Molecular simplification of lipid A structure: TLR4-modulating cationic and anionic amphiphiles. *Mol. Immunol.* 63:153-161; 2015. doi: 10.1016/j.molimm.2014.05.011.

[57] Sawada, K.; Ohtake, T.; Hasebe, T.; Abe, M.; Tanaka, H.; Ikuta, K.; Suzuki, Y.; Fujiya, M.; Hasebe, C.; Kohgo, Y. Augmented hepatic toll-like receptors by fatty acids trigger the pro-inflammatory state of non-alcoholic fatty liver disease in mice. *Hepatol. Res.* 44:920-934; 2014. doi: 10.1111/hepr.12199.

[58] Carotti, S.; Guarino, M. P.; Vespasiani-Gentilucci, U.; Morini, S. Starring role of toll-like receptor-4 activation in the gut-liver axis. *World J. Gastrointest. Pathophysiol.* 6:99-109; 2015. doi: 10.4291/wjgp.v6.i4.99.

[59] Marcolin, E.; San-Miguel, B.; Vallejo, D.; Tieppo, J.; Marroni, N.; Gonzalez-Gallego, J.; Tuñon, M. J. Quercetin treatment ameliorates inflammation and fibrosis in mice with nonalcoholic steatohepatitis. *J. Nutr.* 142:1821-1828; 2012. doi: 10.3945/jn.112.165274.

[60] Tieppo, J.; Cuevas, M. J.; Vercelino, R.; Tuñón, M. J.; Marroni, N. P; González-Gallego J. Quercetin administration ameliorates pulmonary complications of cirrhosis in rats. *J Nutr*. 139(7):1339-46; 2009. doi: 10.3945/jn.109.105353.

[61] Cai, D.; Yuan, M.; Frantz, D. F.; Melendez, P. A.; Hansen, L.; Lee, J.; Shoelson, S. E. Local and systemic insulin resistance resulting from hepatic activation of IKK-beta and NF-kappaB. *Nat. Med.* 11:183-190; 2005. doi: 10.1038/nm1166.

[62] Abdelmegeed, M. A.; Banerjee, A.; Yoo, S. H.; Jang, S.; Gonzalez, F. J.; Song, B. J. Critical role of cytochrome P450 2E1 (CYP2E1) in the development of high fat-induced non-alcoholic steatohepatitis. *J. Hepatol.* 57:860-866; 2012. doi: 10.1016/j.jhep.2012.05.019.

[63] Surapaneni, K. M.; Priya, V. V.; Mallika, J. Pioglitazone, quercetin and hydroxy citric acid effect on cytochrome P450 2E1 (CYP2E1) enzyme levels in experimentally induced non alcoholic steatohepatitis (NASH). *Eur. Rev. Med. Pharmacol. Sci.* 18:2736-2741; 2014.

[64] Farrell, G. C.; van Rooyen, D.; Gan, L.; Chitturi, S. NASH is an inflammatory disorder: Pathogenic, prognostic and therapeutic implications. *Gut Liver* 6:149-171; 2012. doi: 10.5009/gnl.2012.6.2.149.

[65] Byun, E. B.; Yang, M. S.; Choi, H. G.; Sung, N. Y.; Song, D. S.; Sin, S. J.; Byun, E. H. Quercetin negatively regulates TLR4 signaling induced by lipopolysaccharide through tollip expression. *Biochem. Biophys. Res. Commun.* 431:698-705; 2013. doi: 10.1016/j.bbrc.2013.01.056.

[66] Lau, E.; Carvalho, D.; Freitas, P. Gut microbiota: Association with NAFLD and metabolic disturbances. *Biomed. Res. Int.* 2015:979515; 2015. doi: 10.1155/2015/979515.

[67] Memon, R. A.; Bass, N. M.; Moser, A. H.; Fuller, J.; Appel, R.; Grunfeld, C.; Feingold, K. R. Down-regulation of liver and heart specific fatty acid binding proteins by endotoxin and cytokines in vivo. *Biochim. Biophys. Acta* 1440:118-126; 1999. doi:10.1016/S1388-1981(99)00120-1.

[68] Sharifnia, T.; Antoun, J.; Verriere, T. G.; Suarez, G.; Wattacheril, J.; Wilson, K. T.; Peek, R. M.,Jr; Abumrad, N. N.; Flynn, C. R. Hepatic TLR4 signaling in obese

NAFLD. *Am. J. Physiol. Gastrointest. Liver Physiol.* 309:G270-8; 2015. doi: 10.1152/ajpgi.00304.2014.

[69] Lee, J. Y.; Plakidas, A.; Lee, W. H.; Heikkinen, A.; Chanmugam, P.; Bray, G.; Hwang, D. H. Differential modulation of toll-like receptors by fatty acids: Preferential inhibition by n-3 polyunsaturated fatty acids. *J. Lipid Res.* 44:479-486; 2003. doi: 10.1194/jlr.M200361-JLR200.

[70] Rocha, D. M.; Caldas, A. P.; Oliveira, L. L.; Bressan, J.; Hermsdorff, H. H. Saturated fatty acids trigger TLR4-mediated inflammatory response. *Atherosclerosis* 244:211-215; 2016. doi: 10.1016/j.atherosclerosis.2015.11.015.

[71] Neuschwander-Tetri, B. A. Hepatic lipotoxicity and the pathogenesis of nonalcoholic steatohepatitis: The central role of nontriglyceride fatty acid metabolites. *Hepatology* 52:774-788; 2010. doi: 10.1002/hep.23719.

[72] Musso, G.; Gambino, R.; Cassader, M. Cholesterol metabolism and the pathogenesis of non-alcoholic steatohepatitis. *Prog. Lipid Res.*52:175-191; 2013. doi: 10.1016/j.plipres.2012.11.002.

[73] Malhi, H.; Kaufman, R. J. Endoplasmic reticulum stress in liver disease. *J. Hepatol.* 54:795-809; 2011. doi: 10.1016/j.jhep.2010.11.005.

[74] Dandekar, A.; Mendez, R.; Zhang, K. Cross talk between ER stress, oxidative stress, and inflammation in health and disease. *Methods Mol. Biol.* 1292:205-214; 2015. doi: 10.1007/978-1-4939-2522-3_15.

[75] Estadella, D.; da Penha Oller do Nascimento,C.M.; Oyama, L. M.; Ribeiro, E. B.; Damaso, A. R.; de Piano, A. Lipotoxicity: Effects of dietary saturated and transfatty acids. *Mediators Inflamm.* 2013:137579; 2013. doi: 10.1155/2013/137579.

[76] Lewis, M. D.; Roberts, B. J. Role of CYP2E1 activity in endoplasmic reticulum ubiquitination, proteasome association, and the unfolded protein response. *Arch. Biochem. Biophys.* 436:237-245; 2005. doi: 10.1016/j.abb.2005.02.010.

[77] Kim, H. R.; Lee, G. H.; Cho, E. Y.; Chae, S. W.; Ahn, T.; Chae, H. J. Bax inhibitor 1 regulates ER-stress-induced ROS accumulation through the regulation of cytochrome P450 2E1. *J. Cell. Sci.* 122:1126-1133; 2009. doi: 10.1242/jcs.038430.

[78] Rahman, K.; Liu, Y.; Kumar, P.; Smith, T.; Thorn, N. E.; Farris, A. B.; Anania, F. A. C/EBP homologous protein modulates liraglutide-mediated attenuation of non-alcoholic steatohepatitis. *Lab. Invest.* 2016. doi: 10.1038/labinvest.2016.61.

[79] Tobar, N.; Oliveira, A. G.; Guadagnini, D.; Bagarolli, R. A.; Rocha, G. Z.; Araujo, T. G.; Santos-Silva, J. C.; Zollner, R. L.; Boechat, L. H.; Carvalheira, J. B.; Prada, P. O.; Saad, M. J. Diacerhein improves glucose tolerance and insulin sensitivity in mice on a high-fat diet. *Endocrinology* 152:4080-4093; 2011. doi: 10.1210/en.2011-0249.

[80] Gonzalez-Rodriguez, A.; Mayoral, R.; Agra, N.; Valdecantos, M. P.; Pardo, V.; Miquilena-Colina, M. E.; Vargas-Castrillon, J.; Lo Iacono, O.; Corazzari, M.; Fimia, G. M.; Piacentini, M.; Muntane, J.; Bosca, L.; Garcia-Monzon, C.; Martin-Sanz, P.; Valverde, A. M. Impaired autophagic flux is associated with increased endoplasmic reticulum stress during the development of NAFLD. *Cell. Death Dis.* 5:e1179; 2014. doi: 10.1038/cddis.2014.162.

[81] Liu, C. M.; Zheng, G. H.; Ming, Q. L.; Sun, J. M.; Cheng, C. Protective effect of quercetin on lead-induced oxidative stress and endoplasmic reticulum stress in rat liver via the IRE1/JNK and PI3K/akt pathway. *Free Radic. Res.* 47:192-201; 2013. doi: 10.3109/10715762.2012.760198.

[82] Szabo, G.; Csak, T. Inflammasomes in liver diseases. *J. Hepatol.* 57:642-654; 2012. doi: 10.1016/j.jhep.2012.03.035.

[83] Szabo, G.; Petrasek, J. Inflammasome activation and function in liver disease. *Nat. Rev. Gastroenterol. Hepatol.* 12:387-400; 2015. doi: 10.1038/nrgastro.2015.94.

[84] Csak, T.; Ganz, M.; Pespisa, J.; Kodys, K.; Dolganiuc, A.; Szabo, G. Fatty acid and endotoxin activate inflammasomes in mouse hepatocytes that release danger signals to stimulate immune cells. *Hepatology* 54:133-144; 2011. doi: 10.1002/hep.24341.

[85] Ganz, M.; Csak, T.; Szabo, G. High fat diet feeding results in gender specific steatohepatitis and inflammasome activation. *World J. Gastroenterol.* 20:8525-8534; 2014. doi: 10.3748/wjg.v20.i26.8525.

[86] Wang, W.; Wang, C.; Ding, X. Q.; Pan, Y.; Gu, T. T.; Wang, M. X.; Liu, Y. L.; Wang, F. M.; Wang, S. J.; Kong, L. D. Quercetin and allopurinol reduce liver thioredoxin-interacting protein to alleviate inflammation and lipid accumulation in diabetic rats. *Br. J. Pharmacol.* 169:1352-1371; 2013. doi: 10.1111/bph.12226.

[87] Zhang, X.; Zhang, J. H.; Chen, X. Y.; Hu, Q. H.; Wang, M. X.; Jin, R.; Zhang, Q. Y.; Wang, W.; Wang, R.; Kang, L. L.; Li, J. S.; Li, M.; Pan, Y.; Huang, J. J.; Kong, L. D. Reactive oxygen species-induced TXNIP drives fructose-mediated hepatic inflammation and lipid accumulation through NLRP3 inflammasome activation. *Antioxid. Redox Signal.*22:848-870; 2015. doi: 10.1089/ars.2014.5868.

Figure legends

Fig 1. Effect of quercetin on liver histology and lipid accumulation and lipoperoxidation in HFD-fed mice. (A) Representative Haematoxylin & Eosin staining liver sections

from HFD or HFDQ groups, compared with Control (x100). (B) NAFLD activity score (NAS) (calculated from individual scores for steatosis, lobular inflammation and ballooning). (C) Lipid droplets and lipid peroxidation were measured using Bodipy 493/503 (green) and Bodipy 581/591 C_{11} (red), respectively (x100). Nuclei were stained with DAPI (blue). Merged of triple label images are also shown. Photographs shown are representative of 10 animals per group. (D and E) Triglyceride and free fatty acid contents determined as indicated in Materials and Method section. (F) Bar graphs show mRNA levels of CYP2E1 determined by RT-qPCR. Data are described as the means ± SEM (n=10 mice per group). **P<0.01, ***P<0.001 *vs* Control; $^{\#}$P<0.05, $^{\#\#}$P<0.01 *vs* HFD.

Fig 2. Effect of quercetin on lipid metabolism gene expression in HFD-fed mice. (A and B) Bar graphs show mRNA levels of LXRα, SREBP-1c, FAT/CD36, FABP1, FOXA1, C/EBPα and FAS determined by RT-qPCR. (C) Representative western blot of FAS protein expression in liver with 1 sample per group is shown. β-actin levels were used as a loading control. Bar graphs show densitometry analysis of specific bands expressed as percentage relative to Control (100%). Data are described as the means ± SEM of (n=10 mice per group). *P<0.05, **P<0.01, ***P<0.001 vs Control; $^{\#}$P<0.05, $^{\#\#}$P<0.01, $^{\#\#\#}$P<0.001 *vs* HFD.

Fig 3. Effect of quercetin on gut microbiota balance in HFD-fed mice (phylum level). (A) Pie chart showing the differences in bacterial community composition at the phylum level between control and HFD mice with and without supplementation of quercetin. (B) *Firmicutes/Bacteroidetes* ratio of control group and HFD-fed mice with and without quercetin supplementation. The lines between the bars represent significant

differences using the Mann-Whitney U Test. (C) Principal Coordinates Analysis (PCoA) plot derived from the Morisita-Horn dissimilarity index at the phylum level between the four groups. The percentage of the total variance explained is indicated in parenthesis in each axis. Shaded areas denote sample clusters according to diet. (D) Total bacteria concentration analyzed by qPCR between the four groups. Statistical analysis were performed using Kruskal-Wallis followed by Mann-Whitney U test ($P<0.05$).

Fig 4. Effect of quercetin on gut microbiota balance in HFD-fed mice (genus level). Box plot representing the differences between control and HFD mice with and without quercetin at the genus level using The Mann-Whitney U test ($P<0.05$). (A) Box plot showing a higher detection in mice fed with HFD in comparison to the control group. (B) Box plot representing the differences in *Helicobacter* genus detection between control group and HFD-fed mice group with and without quercetin supplementation. (C) Box plot showing a lower detection in HFD group in comparison to the control group.

Fig 5. Effect of quercetin on SCFAs production and intestinal barrier integrity in HFD-fed mice. (A) SCFAs (acetate, propionate and butyrate) levels were measured in caecal samples by gas chromatography-mass spectrometry (GC-MS). (B) Representative western blot of claudin 1, occludin and intestinal alkaline phosphatase (IAP) protein expression in small intestine with 1 sample per group is shown. β-actin levels were used as a loading control. Bar graphs show densitometry analysis of specific bands expressed as percentage relative to Control (100%). Data are described as the means ± SEM of

(n=10 mice per group). **P<0.01, ***P<0.001 *vs* Control; $^{\#}$P<0.05, $^{\#\#}$P<0.01, $^{\#\#\#}$P<0.001 *vs* HFD.

Fig 6. Effect of quercetin on endotoxemia and TLR-4-NF-κB signaling pathway activation in HFD-fed mice. (A) Plasma LPS and ethanol levels were measured using the LAL Chromogenic Endotoxin Quantitation Kit and the colorimetric Ethanol Assay Kit, respectively. (B) Bar graphs show mRNA levels of TLR-4 determined by RT-qPCR (upper panel). Representative western blot of TLR-4 protein expression in liver with 1 sample per group is shown (lower panel). β-actin levels were used as a loading control. Bar graphs show densitometry analysis of specific bands expressed as percentage relative to Control (100%). (C) NF-κB activation was measured by quantification of nuclear and cytosolic p65 levels. Representative western blots with 1 sample per group are shown. Lamin A and β-actin levels were used as a loading control of nuclear and cytosolic p65, respectively. Bar graphs show densitometry analysis of specific bands expressed as percentage relative to Control (100%). (D) Bar graphs show mRNA levels of TNF-α and IL-6 determined by RT-qPCR. Data are described as the means ± SEM of (n=10 mice per group). **P<0.01, ***P<0.001 *vs* Control; $^{\#}$P<0.05, $^{\#\#}$P<0.01, $^{\#\#\#}$P<0.001 *vs* HFD.

Fig. 7. Effect of quercetin on inflammasome activation and ER stress pathway induction in HFD-fed mice. (A) NLRP3 inflammasome and its downstream pathway activation. Left panel: Bar graphs show mRNA levels of NLRP3 and caspase 1 determined by RT-qPCR. Right panel: Representative western blots of NLRP3 and active caspase 1 protein expression in liver with 1 sample per group are shown. β-actin levels were used as a loading control. Bar graphs show densitometry analysis of specific bands expressed as

percentage relative to Control (100%). (B) Reticulum stress pathway activation. Left panel: Bar graphs show mRNA levels of ER stress markers GRP78 and CHOP determined by RT-qPCR. Right panel: Representative western blots of GRP78 and CHOP protein expression in liver with 1 sample per group are shown. β-actin levels were used as a loading control. Bar graphs show densitometry analysis of specific bands expressed as percentage relative to Control (100%). Data are described as the means ± SEM of (n=10 mice per group). **P<0.01, ***P<0.001 *vs* Control; $^{\#}$P<0.05, $^{\#\#}$P<0.01, $^{\#\#\#}$P<0.001 *vs* HFD.

Fig. 8. Modulation of intestinal microbiota imbalance and related gut-liver axis activation by quercetin improves HFD-induced NAFLD in mice. The protective effect of quercetin is mediated by dysbiosis-induced TLR-4-NF-κB signaling pathway activation and FFA and CYP2E1-dependent lipotoxicity blockage, counteracting inflammasome initiation response as well as reticulum stress pathway induction. This integrated antioxidant, anti-inflammatory and prebiotic effect of quercetin treatment leads to the improvement of lipid metabolism deregulation implicated in HFD-driven NAFLD development.

Fig 1S. Principal Coordinates Analysis (PCoA) plot derived from the Morisita-Horn dissimilarity index at the genus level among control group with (ControlQ) and without quercetin (Control) and HFD-fed mice supplemented with (HFDQ) or without quercetin (HFD). The percentage of the total variance explained is indicated in parenthesis in each axis. Shaded areas denote sample clusters according to diet. Dashed lines show the HFD-fed mice supplemented with quercetin subset.

Fig. 2S. NAFLD activity score (NAS) correlated with *Firmicutes/Bacteroidetes* ratio and total bacteria concentration. (A) Correlation between NAS and *Firmicutes/Bacteroidetes* ratio, (B) Correlation between NAS and total bacteria concentration (ng/µl) of control mice (Control), control-fed mice supplemented with quercetin (ControlQ), HFD-fed mice (HFD) and HFD-fed mice supplemented with quercetin (HFDQ) for 16 weeks. Pearson's r correlation and corresponding P value were shown.

Table 1. Bacterial 16S rRNA gene primers used for real-time PCR.

Target Group	**Primer name**	**Sequence (5´-3´)**	**Annealing Temperature (ºC)**
All bacteria (Universal)	926F 1062R	AAACTCAAAKGAATTGACGG CTCACRRCACGAGCTGAC	59ºC

Table 2. Primers and probes used for the RT-qPCR.

Gene	Genbank	Assay ID	Amplicon size	Dye
LXRα	NM_001177730.1	Mm00443454_m1	79	FAM™
SREBP-1c	NM_011480.3	Mm00550338_m1	62	FAM™
FAT/CD36	NM_001159555.1	Mm01135198_m1	112	FAM™
FAS	NM_007988.3	Mm00662319_m1	67	FAM™
FABP1	NM_017399.4	Mm00444340_m1	72	FAM™
FOXA1	NM_008259.3	Mm00484713_m1	68	FAM™
C/EBPα	NM_007678.3	Mm00514283_s1	99	FAM™
TLR-4	NM_021297.2	Mm00445273_m1	87	FAM™
IL-6	NM_031168.1	Mm00446190_m1	78	FAM™
TNF-α	NM_001278601.1	Mm00443258_m1	81	FAM™
NLRP3	NM_145827.3	Mm00840904_m1	84	FAM™
Caspase 1	NM_009807.2	Mm00438023_m1	99	FAM™
GRP78	NM_001163434.1	Mm00517691_m1	75	FAM™
CHOP	NM_007837.4	Mm00492097_m1	82	FAM™
CYP2E1	NM_021282.2	Mm00491127_m1	83	FAM™
GAPDH	NM_008084.2	4352339E	107	VIC™

LXRα, liver X receptor alpha; SREBP-1c, sterol regulatory element binding protein 1c; FAT/CD36, fatty acid translocase CD36; FAS, fatty acid synthase; FABP1, fatty acid binding protein 1; FOXA1, forkhead box protein A1; C/EBPα, CCAAT/enhancer binding protein alpha; TLR-4, toll-like receptor 4; IL-6, interleukin 6; TNF-α; tumor necrosis factor; NLRP3, NOD-like receptor family pyrin domain containing 3; GRP78, 78 kDa glucose-regulated protein; CHOP, CCAAT-enhancer-binding protein homologous protein; CYP2E1, cytochrome P450 2E1; GAPDH, glyceraldehyde-3-phosphate dehydrogenase.

Table 3. Effect of quercetin on metabolic syndrome-related parameters in mice fed a high-fat diet for 16 weeks.

	Control	HFD	HFDQ
Body weight gain (g)	9.2 ± 0.4	22.2 ± 2.3***	17.2 ± 2.1**$^{\#}$
Liver weight (g)	1.5 ± 0.1	1.8 ± 0.3*	1.5 ± 0.1$^{\#}$
Epididymal fat pads (% of body weight)	1.6 ± 0.1	6.2 ± 0.2***	4.3 ± 0.1**$^{\#\#\#}$
Food intake (g/day)	3.3 ± 0.1	2.9 ± 0.1*	2.9 ± 0.1*
Fasting glycemia (mg/dl)	111.7 ± 7.3	170.6 ± 18***	154.8 ± 12**$^{\#}$
Fasting insulinemia (ng/ml)	0.4 ± 0.4	1.6 ± 0.5***	1.1 ± 0.2$^{\#\#}$
HOMA-IR	2.7 ± 1.6	17.2 ± 2.8***	11 ± 1.5**$^{\#\#}$
ALT (U/l)	21.8 ± 2.3	67.1 ± 16**	43.3 ± 4.8$^{\#}$
TG (mg/dl)	25.2 ± 2.5	36.8 ± 1.8**	26.6 ± 3.1$^{\#\#}$
IL-6 (pg/ml)	27.6 ± 2.0	102 ± 6.9***	76 ± 5.2***$^{\#\#}$

Data are means ± SEM (n=6 mice per group). *p<0.05, **p<0.01, ***p<0.001 *vs* Control; $^{\#}$p<0.05, $^{\#\#}$p<0.01, $^{\#\#\#}$p<0.001 *vs* HFD. ALT, alanine aminotransferase; HOMA-IR, homeostasis model assessment of insulin resistance; TG, triglycerides.

Figure 1

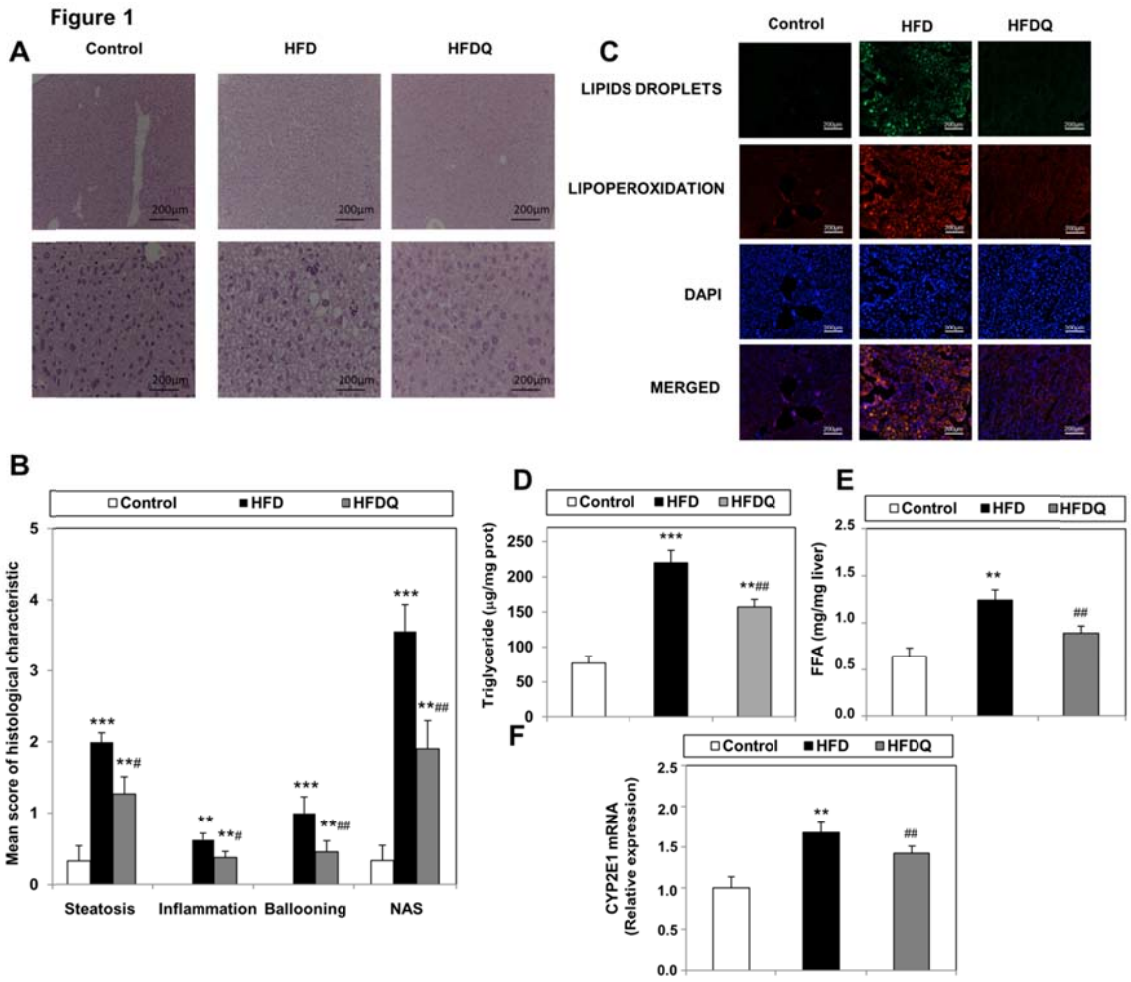
A
Control
HFD
HFDQ
200µm
C
Control
HFD
HFDQ
LIPIDS DROPLETS
LIPOPEROXIDATION
DAPI
MERGED
B
Control
HFD
HFDQ
Mean score of histological characteristic
Steatosis
Inflammation
Ballooning
NAS
D
Triglyceride (µg/mg prot)
E
FFA (mg/mg liver)
F
CYP2E1 mRNA (Relative expression)

Figure 2

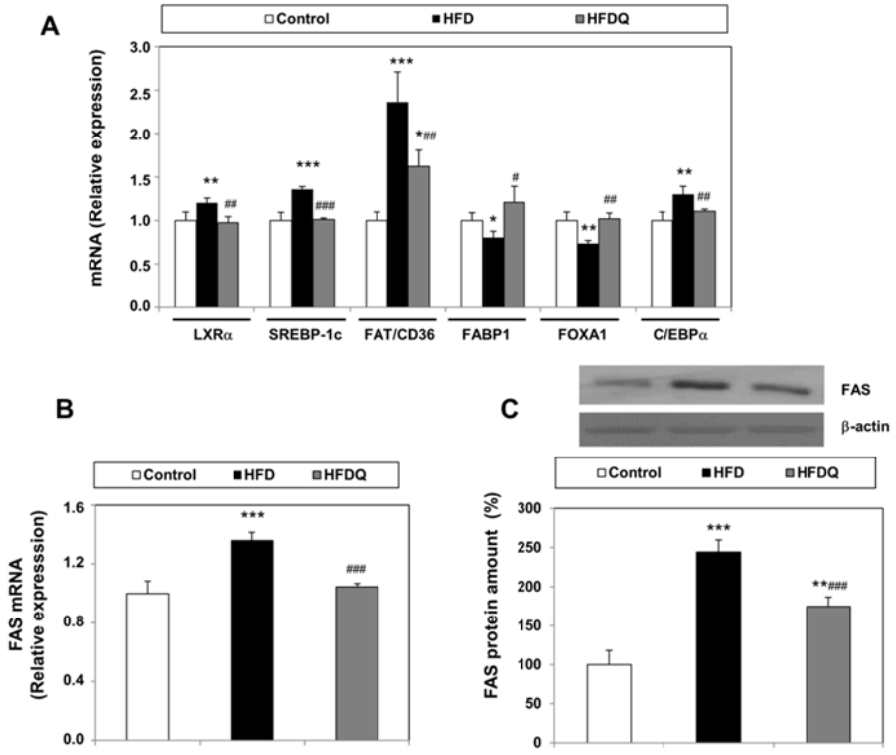
A
Control
HFD
HFDQ
mRNA (Relative expression)
3.0
2.5
2.0
1.5
1.0
0.5
0.0
LXRα
SREBP-1c
FAT/CD36
FABP1
FOXA1
C/EBPα
B
FAS mRNA
(Relative expresssion)
1.6
1.2
0.8
0.4
0.0
C
FAS
β-actin
FAS protein amount (%)
300
250
200
150
100
50
0

Figure 3

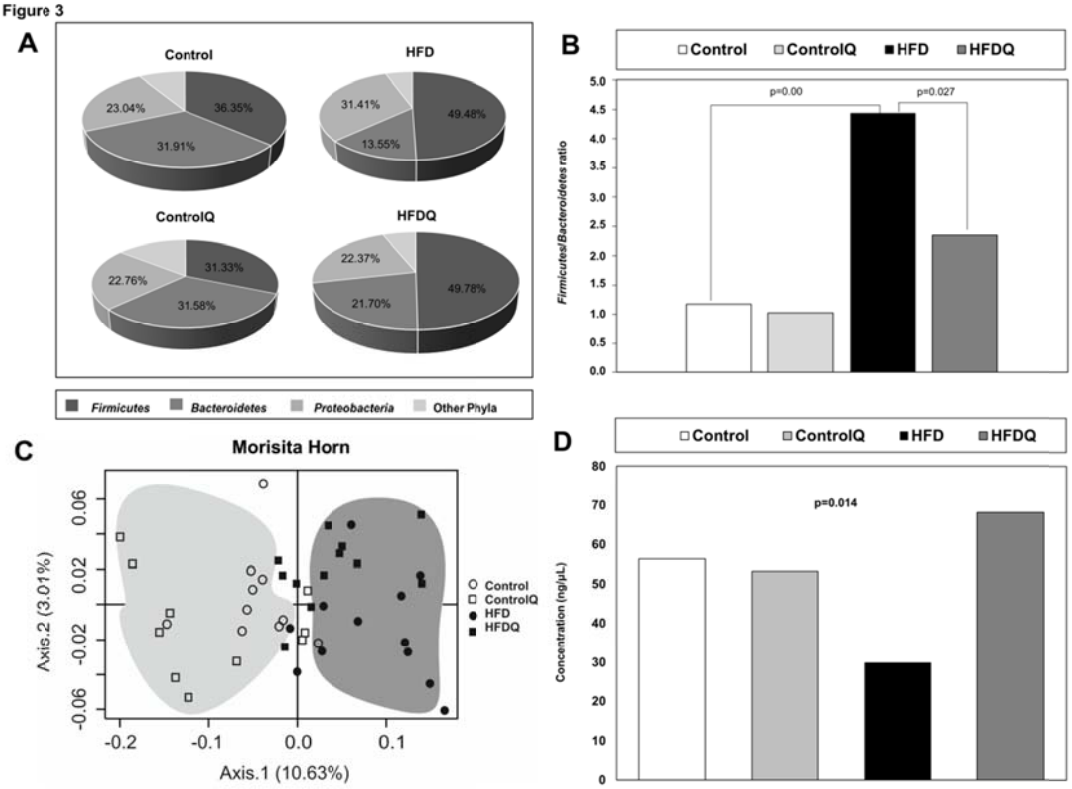
A
Control
HFD
ControlQ
HFDQ
36.35%
23.04%
31.91%
49.48%
31.41%
13.55%
31.33%
22.76%
31.58%
49.78%
22.37%
21.70%
Firmicutes
Bacteroidetes
Proteobacteria
Other Phyla
B
Control
ControlQ
HFD
HFDQ
p=0.00
p=0.027
Firmicutes/Bacteroidetes ratio
C
Morisita Horn
Axis.2 (3.01%)
Axis.1 (10.63%)
Control
ControlQ
HFD
HFDQ
D
Control
ControlQ
HFD
HFDQ
p=0.014
Concentration (ng/µL)

Figure 4

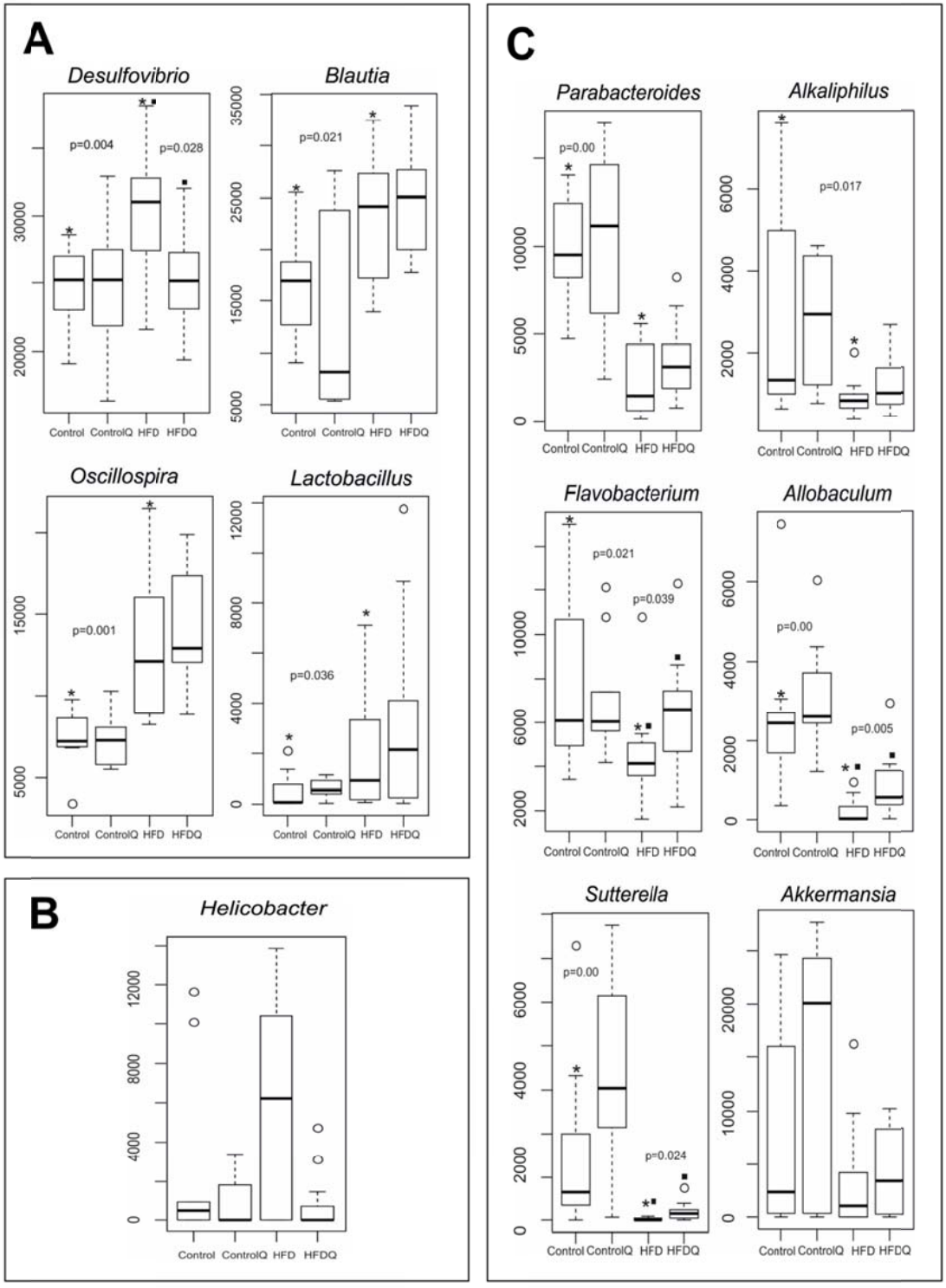
A
Desulfovibrio
p=0.004
p=0.028
Blautia
p=0.021
Oscillospira
p=0.001
Lactobacillus
p=0.036
B
Helicobacter
C
Parabacteroides
p=0.00
Alkaliphilus
p=0.017
Flavobacterium
p=0.021
p=0.039
Allobaculum
p=0.00
p=0.005
Sutterella
p=0.00
p=0.024
Akkermansia
Control ControlQ HFD HFDQ

Figure 5

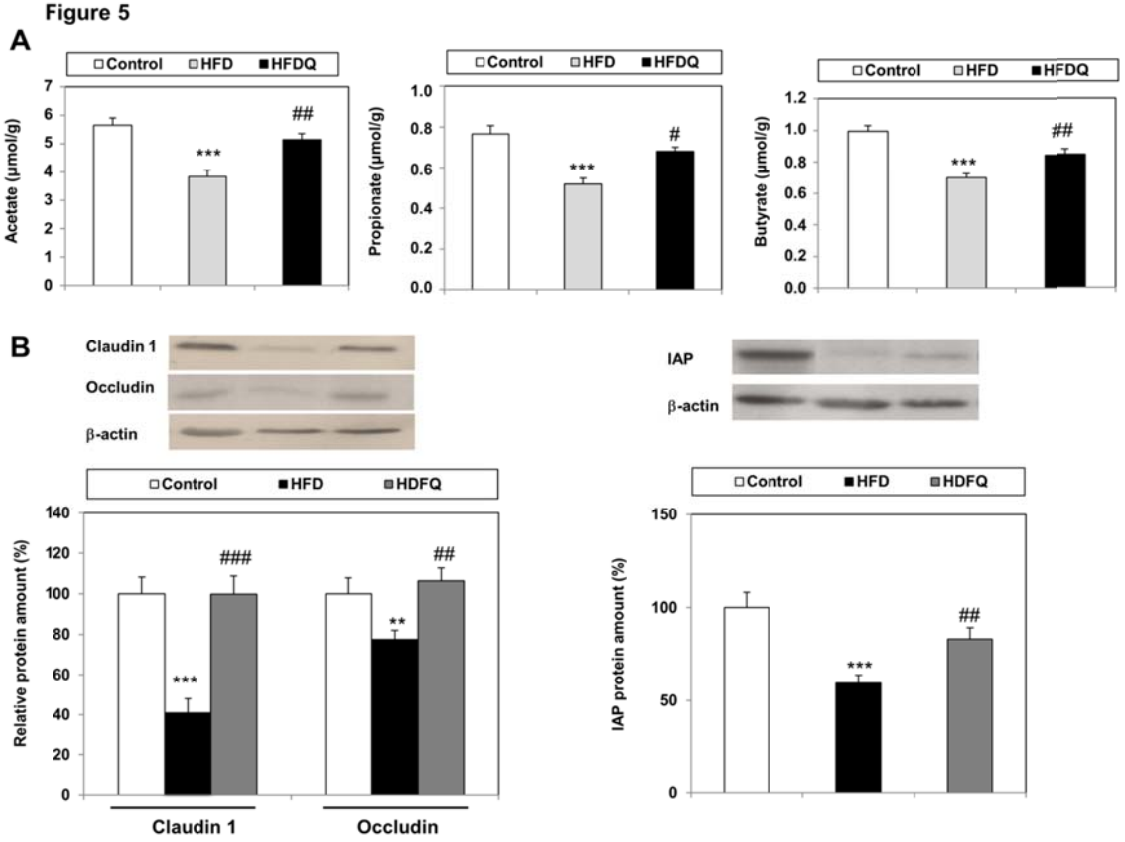
A
Control
HFD
HFDQ
Acetate (μmol/g)
Propionate (μmol/g)
Butyrate (μmol/g)
***
##
#
B
Claudin 1
Occludin
β-actin
IAP
Control
HFD
HDFQ
Relative protein amount (%)
IAP protein amount (%)
###
**
Claudin 1
Occludin

Figure 6

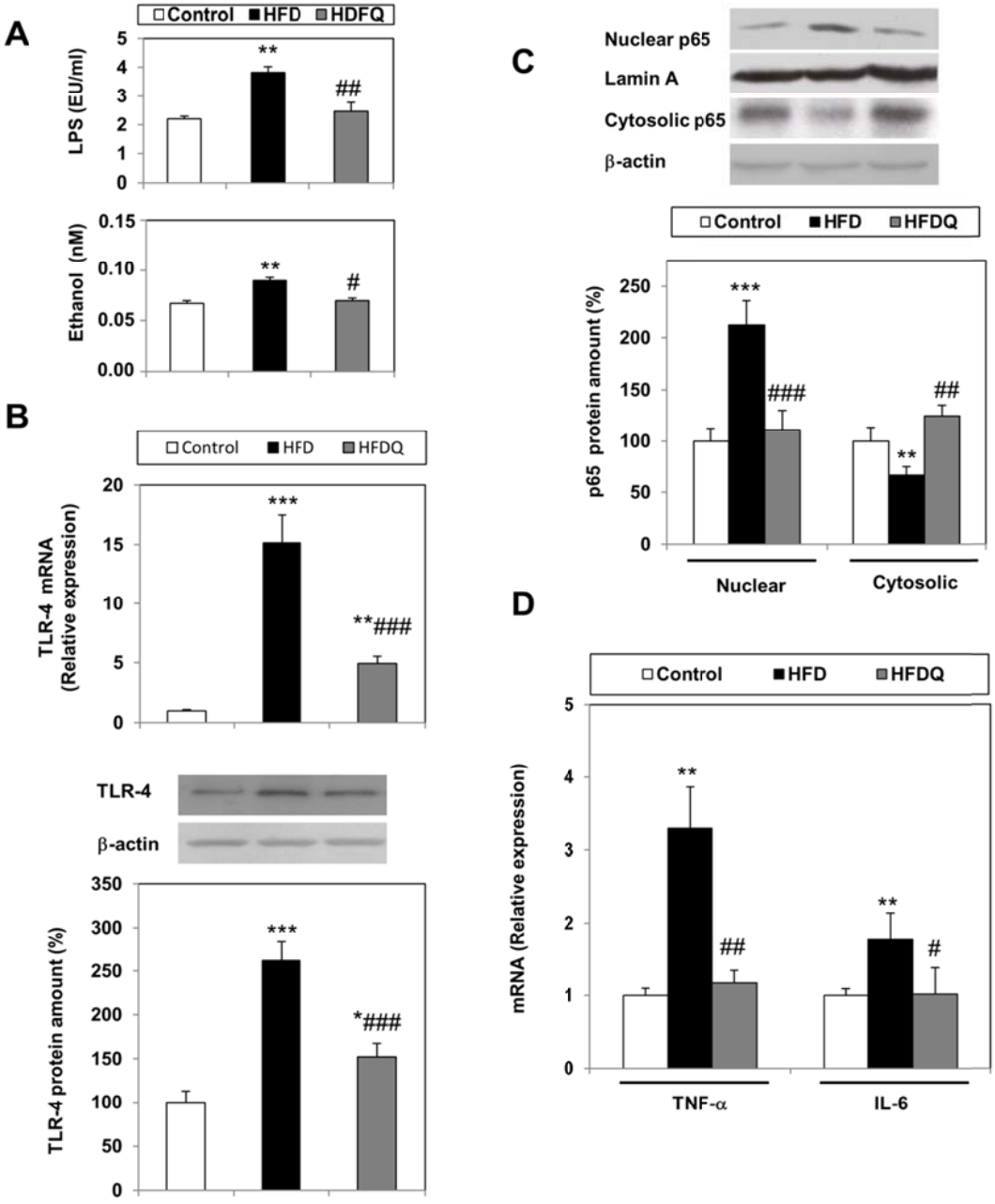
A
Control
HFD
HDFQ
LPS (EU/ml)
Ethanol (nM)
B
TLR-4 mRNA (Relative expression)
TLR-4
β-actin
TLR-4 protein amount (%)
C
Nuclear p65
Lamin A
Cytosolic p65
β-actin
p65 protein amount (%)
Nuclear
Cytosolic
D
mRNA (Relative expression)
TNF-α
IL-6

Figure 7

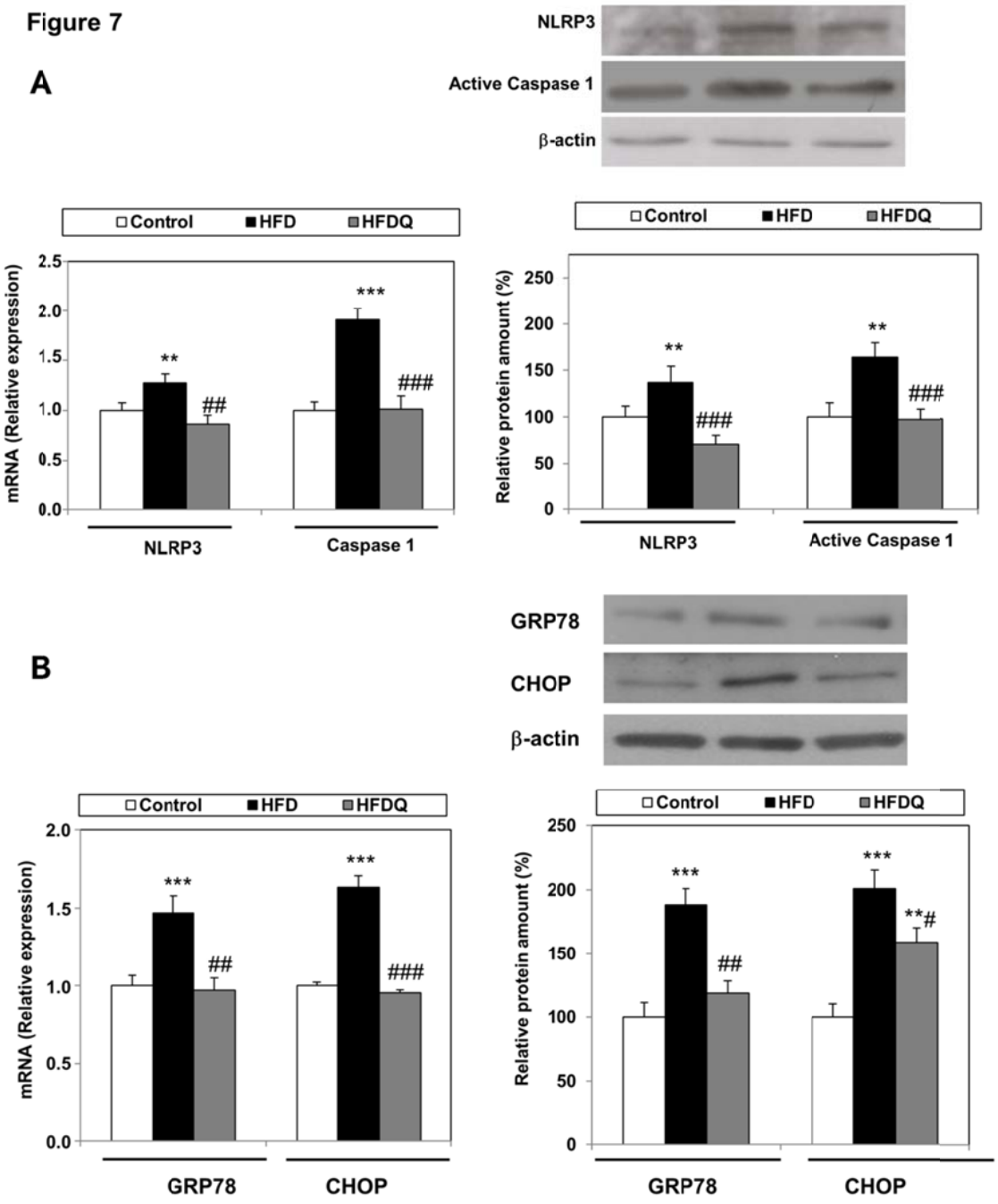
A
NLRP3
Active Caspase 1
β-actin
Control
HFD
HFDQ
mRNA (Relative expression)
Relative protein amount (%)
NLRP3
Caspase 1
Active Caspase 1
B
GRP78
CHOP
β-actin

Figure 8

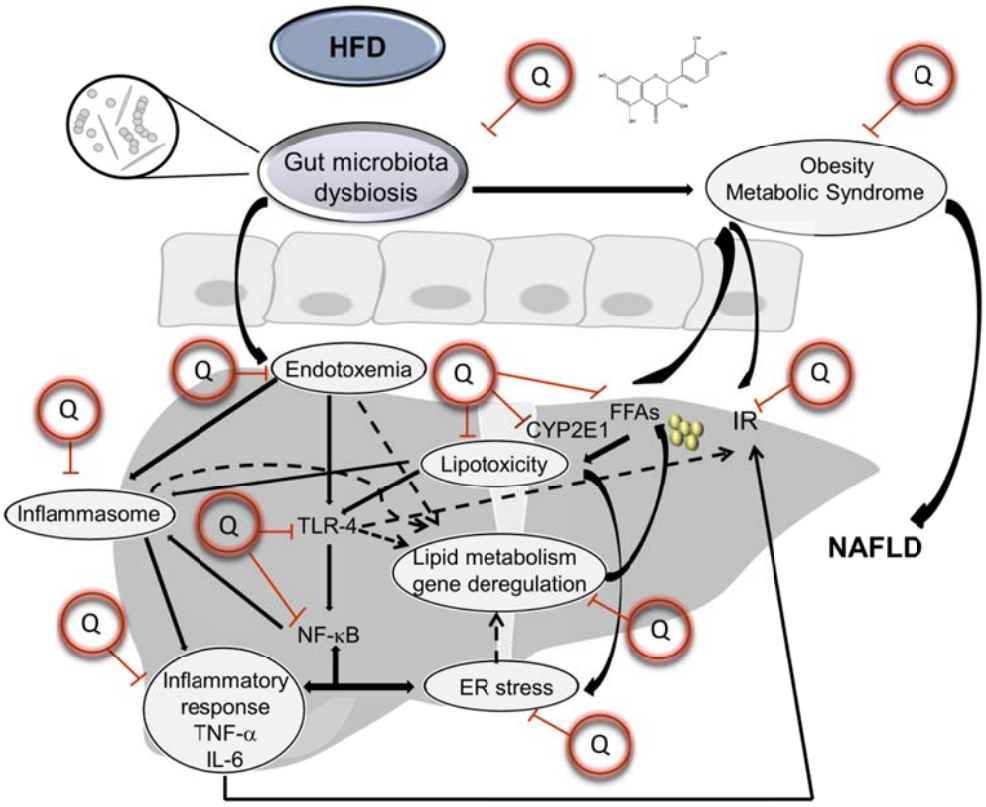
HFD
Q
Gut microbiota dysbiosis
Obesity Metabolic Syndrome
Endotoxemia
CYP2E1
FFAs
IR
Lipotoxicity
Inflammasome
TLR-4
Lipid metabolism gene deregulation
NAFLD
NF-κB
Inflammatory response TNF-α IL-6
ER stress

Figure S1

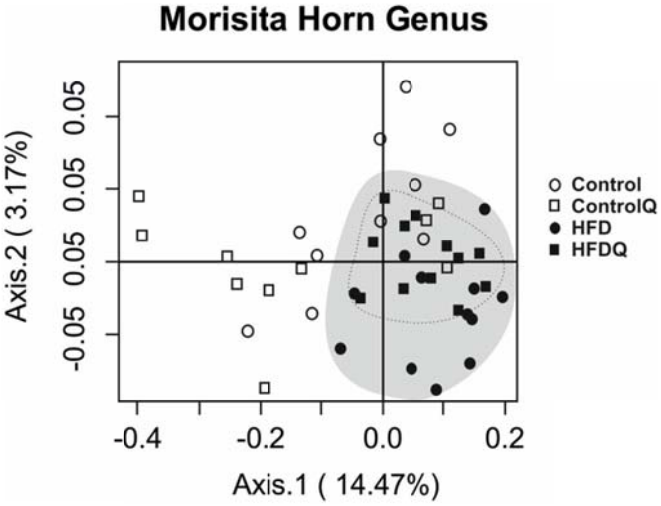
Morisita Horn Genus
Axis.2 (3.17%)
0.05
0.05
0.05
-0.05
-0.4
-0.2
0.0
0.2
Axis.1 (14.47%)
Control
ControlQ
HFD
HFDQ

Figure S2

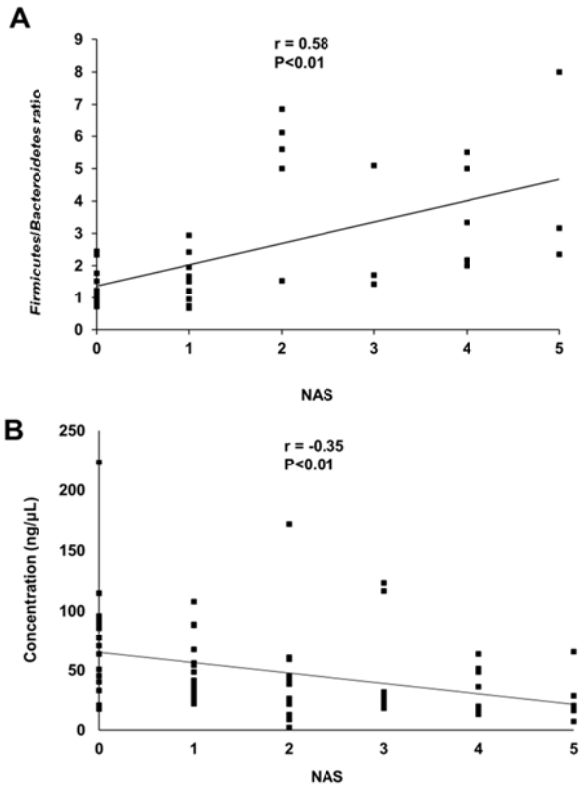
A
r = 0.58
P<0.01
Firmicutes/Bacteroidetes ratio
NAS
B
r = -0.35
P<0.01
Concentration (ng/µL)
NAS